Virginia Commonwealth University
VCU Scholars Compass

Master of Science in Forensic Science Directed Research Projects

Dept. of Forensic Science

2021

Qualitative and Quantitative Characterization of Epithelial Cell Mixtures Using Hormone Antibody Probes and Flow Cytometry

Luke Baldridge
Virginia Commonwealth University

Follow this and additional works at: https://scholarscompass.vcu.edu/frsc_projects

 Part of the Biology Commons

© The Author(s)

Downloaded from
https://scholarscompass.vcu.edu/frsc_projects/21

This Directed Research Project is brought to you for free and open access by the Dept. of Forensic Science at VCU Scholars Compass. It has been accepted for inclusion in Master of Science in Forensic Science Directed Research Projects by an authorized administrator of VCU Scholars Compass. For more information, please contact libcompass@vcu.edu.

© Luke “Isaac” Baldridge 2021

All Rights Reserved

QUALITATIVE AND QUANTITATIVE CHARACTERIZATION OF EPITHELIAL CELL MIXTURES USING HORMONE ANTIBODY PROBES AND FLOW CYTOMETRY

A thesis submitted in partial fulfillment of the requirements for the degree of Master of Science at Virginia Commonwealth University

by

LUKE “ISAAC” BALDRIDGE

Bachelor of Science, Kent State University, 2019

Summer 2020 - Spring 2021

Virginia Department of Forensic Science, Richmond, VA

Research Mentor: Dr. Susan Greenspoon

Submitted Spring 2021

Acknowledgements

The author wishes to thank multiple people. I would like to thank my research mentor Dr. Susan Greenspoon and my committee members Dr. Christopher Ehrhardt, and Dr. William Eggleston. Thank you to Dr. Ehrhardt for welcoming me into his lab to Dr. Greenspoon for allowing me the experience of interning at the Virginia Department of Forensic Science. Thank you to all three of my committee members for always pushing me and providing me with a wealth of feedback. I would like to acknowledge Dr. Sarah Ingram for being my sounding board for this project, for which I am very grateful. Thank you to my parents, Leann and Ray Baldridge, for their financial and emotional support that helped me accomplish more than I ever could have dreamed of accomplishing alone. I would also like to thank my partner Abbey Grapperhaus for loving and believing in me through thick and thin, even when our time together was scattered and sparse at times.

Abstract

"Touch" DNA is evidence that consists of epidermal cells deposited by handling objects and it is becoming more common in evidence samples processed in crime labs. Because "touch" DNA evidence samples may be low-template DNA and are often mixtures, there is a need to both nondestructively estimate the amount of DNA present prior to DNA purification and to identify and characterize mixtures prior to DNA typing. The purpose of this study was to test the use of FITC-labeled anti-testosterone antibodies as a potential tool to estimate the number of contributors in two-, three-, and four-person mixtures of epidermal skin cells, as well as estimate the quantity of DNA in single-source epidermal cells. DNA mixture profiles can be difficult to interpret and any information prior to profile generation may aid in developing the most informed interpretation of the data. Single-source and mixture samples bound to anti-testosterone antibodies were assessed for their fluorescent intensities using a Guava® easycyte™ flow cytometer. Only some of the two- (3/18) and three-person (1/9) mixture fluorescence histograms correctly estimated the number of contributors but none of the four-person (0/3) mixtures were successful. Statistical analysis of single-source and mixture histogram distribution demonstrated some capability of predicting the presence of a mixture but requires further testing. To predict DNA content, stained single-source samples were collected from the flow cytometer and subjected to DNA extraction and quantification. Plotting of median fluorescent intensity against the DNA quantity of single-source donors revealed no apparent correlation, though most DNA quantities were not reliably detected. To provide support to the mixture and DNA quantity studies, the specificity of the anti-testosterone antibody was assessed by comparing its fluorescent intensity to a FITC-labeled non-specific isotype control. The anti-testosterone antibody demonstrated a substantially greater fluorescent intensity indicative of greater antibody binding and was determined to be more specific than the isotype control. To optimize fluorescent intensity for future studies, single-source samples were stained with anti-testosterone and FITC-labeled anti-dihydrotestosterone antibodies together at various volumes [2.5, 5, and 10 uL]. The optimal combination of the two antibodies may be 2.5 uL anti-testosterone and 10 uL anti-dihydrotestosterone but requires more testing. This study demonstrates that anti-testosterone antibodies have the potential to be used in a nondestructive technique to estimate the number of contributors in a mixture of epidermal skin cells by specific staining but may not be able to estimate DNA quantity in single-source samples.

Key words: Forensic Science, Touch DNA, DNA Mixtures, Flow Cytometry, Testosterone, Dihydrotestosterone, Epidermal Skin Cells

Introduction

In recent years, forensic cases have had an increase in crime scene evidence from handled items (also referred to as touch DNA evidence) (1). Approximately half of all contemporary casework is comprised of touch DNA evidence (1). While touch DNA is not always low template, the analysis is frequently complicated by low levels of DNA derived from mostly anucleate and highly keratinized epidermal cells which makes up the first two layers of the epidermis (stratum corneum and stratum lucidum) (2, 3, 4). A large proportion of the DNA obtained from samples comprised primarily of these keratinized cells may be extracellular DNA (eDNA). (5, 6). Because eDNA exists outside of the cell, a large portion of the DNA from touch evidence is exposed to harsh conditions in the environment that can severely degrade DNA such as heat, oxygen, or ultraviolet (UV) light (7). Degraded DNA in short tandem repeat (STR) profiles can result in allele drop-out, or full locus drop-out (8). Low-template DNA (LT-DNA) can result in allele drop-in due to frequent contamination of DNA of very low levels (8). Additionally, many touch DNA samples are mixtures of multiple contributors due to many people handling the same object, and the frequency of mixture detection in crime scene evidence has increased over the years due to more sensitive STR kits (8, 9). All of these factors further complicate downstream DNA analysis and can sometimes make contributor specific allele attribution nearly impossible.

There are numerous methods currently used in forensic science to identify and analyze mixtures, though they each have their limitations. An indirect method of detecting the presence of a mixture is by using a physical evidence recovery kit (PERK) to collect potential DNA evidence on a swab from a female victim. It is possible to presumptively detect seminal fluid or microscopically identify sperm cells on the swab; because specific male components are

indicated or identified on a female victim, a mixture of male and female DNA is implied (10). It should be noted that this mixture detection method must use male specific components like seminal fluid or sperm cells to successfully indicate a mixture. This method does not offer detection of touch DNA evidence mixtures from epidermal skin cells, even if one or more contributors are male. This method also only detects male:female mixtures when seminal fluid from a non-vasectomized male has been deposited and cannot identify same sex mixtures, nor estimate the number of contributors.

Another common mixture identification method is during the DNA quantification step in the forensic DNA analysis workflow. While these are not the only examples, the PowerQuant® and Quantifiler™ Trio quantification systems can indicate the presence of a mixture by calculating the ratio of male DNA to total human DNA. This is possible because both systems quantify DNA using an autosomal DNA target and a *Y-chromosome* DNA target during quantitative PCR (qPCR) (11, 12). This method is not restricted to a particular cell type because most male cells will have a *Y-chromosome* (except for *X-chromosome* containing sperm cells), and the ratio of male to total human DNA gives an indication as to how much DNA was contributed by the male and female contributors. However, this method requires evidence sample destruction to be performed, cannot identify same sex mixtures, and cannot indicate the number of contributors to the mixture.

The last commonly used method of mixture identification is performed during STR profile interpretation. Similar to the DNA quantification method, it is sometimes possible to identify major and minor contributors based on allele peak heights but is not always the case in mixtures of equal amounts of DNA from each contributor. Assessing the STR profiles for the number of contributors to a mixture becomes increasingly less accurate as mixture complexity

dramatically increases once there are more than three contributors to the sample (13-18). Although it is also sometimes possible to identify the number of contributors by the largest number of alleles observed at a single locus, it may not always be useful in touch DNA evidence that could also be LT-DNA and/or degraded DNA and the many complicating factors that come with this type of evidence. Similar to the DNA quantification method, STR profiling requires sample consumption which can be problematic if there is not enough sample to save for retesting at a later time, which is always desirable in forensic evidence analysis. This method is also time consuming because it requires that the DNA sample undergo the entire forensic DNA workflow to the completion of STR profile interpretation.

Many of these methods are incapable of estimating the number of contributors in a touch DNA sample, identifying same sex mixtures, and all of these methods are unable to estimate the quantity of DNA without sample destruction. This gives rise to the need for a new approach to nondestructively identify the number of contributors in a mixture whether they are same or different sexes, and to estimate the quantity of DNA prior to sample destruction. This approach could save time and resources by identifying whether a probative mixture is present in evidence or if the estimated DNA quantity is high enough to move forward with DNA quantification and STR profiling on the sample. One potential method to achieve these goals uses fluorescently labeled antibody probes to differentially stain epidermal skin cells for the target molecules testosterone and dihydrotestosterone and to detect differences in levels of fluorescence between multiple individuals via flow cytometry.

Testosterone is a cholesterol-based molecule that is fat soluble and passively diffuses across cell membranes of target tissues such as muscle, bone, fat, liver, skin, and myeloid tissues (19). Approximately 10% of testosterone is reduced to the androgen molecule

dihydrotestosterone (DHT) in the skin by the enzyme 5α-reductase (20). Both testosterone and DHT are able to bind an androgen receptor complex in the cytoplasm of target cells, NR3C4 (nuclear receptor sub family 3, group C, member 4), after which the hormone-androgen receptor complex is then transported to the nucleus (21). Testosterone that does not interact with target tissues is metabolized by the liver (22, 23). In addition to the liver, testosterone is metabolized in the kidney, gut, muscle, and adipose tissues by hepatic oxidases, notably cytochrome P-450 3A family (24). There is little information on whether testosterone is also metabolized in non-target tissues or it passively diffuses out of the cell until it reaches a target tissue or is metabolized elsewhere. Testosterone and dihydrotestosterone are prevalent signaling molecules in many tissues including epithelial cells (25, 26), which make them promising target molecules for touch DNA evidence. It has also been observed that testosterone is a stable molecule, maintaining consistent levels in stored serum for over 40 years (27). This supports the possibility that it may act as a biomarker that does not degrade as easily in forensically related samples that are commonly subjected to harsh environmental conditions and degradation.

A previous study used fluorescently labeled anti-testosterone and anti-dihydrotestosterone antibodies to stain epidermal skin cell populations from male-female mixtures and successfully enhanced for male and female DNA profiles after cell separation of the stained mixture into male and female fractions using fluorescently activated cell sorting (FACS) (28). Testosterone and dihydrotestosterone were chosen as markers in this previous study because they are more abundant in males than in females; the prevalence of testosterone in blood serum is about 10 times that of the levels in females (27, 29, 30), and that disparity was hypothesized to potentially translate to other tissues like epidermal skin cells. This was intended to serve as a method of discriminating between male and female cells via fluorescently labeled

anti-testosterone and anti-dihydrotestosterone antibodies. However, one major observation of the Miller et al. (2019) study was that male epidermal skin cells were not consistently labeled at a higher signal compared to female cells (28). This key finding supports the current hypothesis that fluorescent signals from epidermal skin cell staining differ in individuals rather than only showing the previously hypothesized differences between females with a low signal and males with a high signal. This allows for the testing of differential staining of epidermal skin cells using testosterone and DHT as antibody targets and anti-testosterone (anti-T) and anti-dihydrotestosterone (anti-DHT) antibodies as the fluorescently labeled probes to resolve touch/epidermal skin cell mixtures via flow cytometry. Because testosterone is a macromolecule prevalent in the skin, it is hypothesized that samples with a large amount of fluorescence due to antibody binding will likely have a greater amount of DNA because testosterone and DNA are both macromolecules.

Flow cytometry is a process that allows cells to move through a capillary small enough that the cells must move in a single-file line as they pass by a laser of a specific wavelength that excites the fluorophores attached to the antibodies bound to the cells (31). There are detectors inside of the instrument in order to capture the emitted fluorescence wavelength from the fluorophores before it is digitized for analysis (31). The cell size and complexity are also determined by detectors that capture the scattered light from the laser that interrogates the cells. The forward scatter light measures cell size, and the side scatter light in the perpendicular direction measures cell complexity. There are bandpass filters in front of the detectors to ensure that none of the light from the laser enters the detectors, only the scattered light and fluorescent emissions of the fluorophores. The bench top instrument Guava® easyCyte™ flow cytometer (Millipore Inc., Burlington, MA) can be utilized in forensic science research for the collection of

data regarding the relative fluorescence of cell populations to generate fluorescence histograms. The Guava flow cytometer is simple and efficient; however, the instrument is limited in that each sample must be analyzed one at a time and does not offer high-throughput capabilities.

In this study, epidermal skin cells were used because they served as a mean of replicating touch DNA evidence. Additionally, touch DNA evidence is frequently composed of multiple contributors and can have low levels of DNA, which often confounds STR profile interpretation (8, 9). Thus, anti-testosterone antibody (anti-T) binding to epidermal skin cells was tested to determine if it could be used to nondestructively estimate the number of contributors in mixture samples by identifying the number of distinguishable peaks in fluorescence histograms of mixture samples. A number of tests were performed in order to assess the use labeled anti-hormone antibodies for epithelial touch sample characterization. In order to estimate DNA quantity, the median fluorescence of single-source samples was plotted against DNA concentration to determine if a correlation existed. The specificity of the anti-testosterone antibody was explored by comparing its staining pattern and level of fluorescence to an isotype control antibody, which is used to determine the level of non-specific binding present during probe hybridizations. The anti-testosterone and anti-DHT antibodies were optimized together to produce the greatest shift in fluorescence. Finally, two-, three- and four-person epidermal cell mixtures were created and assessed for contributor number by plotting the fluorescent signal patterns.

Applications of antibody staining such as resolving touch mixtures or utilizing the extent of probe binding to predict the quantity of recoverable DNA in the sample have had some advancement but could be explored further. The first goal of this project was to optimize epidermal cell staining using fluorescently labeled antibodies complementary to testosterone and

dihydrotestosterone (DHT) because both macromolecules are thought to exist in the epidermal skin cells. These probes were then used to stain skin epithelial cells from touch/trace mixtures and single-source samples to generate fluorescence histograms using flow cytometry. This epidermal cell staining method was used to pursue a number of objectives: I.) to confirm the specificity of anti-T probes by comparing fluorescent intensity with isotype control fluorescent intensity to determine if anti-T was noticeably more fluorescent, II.) to evaluate the number of contributors to two-, three-, and four-person mixtures and determine if the number of distinguishable peaks in the fluorescence histogram staining pattern accurately and reproducibly reflected the contributor number, III.) to optimize staining with anti-T and anti-DHT probes together in single-source samples for greater fluorescent intensity by varying the volumes of each probe added, and IV.) to determine if there is a correlation between the quantity of recoverable DNA and the median fluorescent intensity in single-source samples and use the model to accurately predict DNA quantities nondestructively.

Methods

Sample Collection

Multiple sampling methods were performed in order to maximize cell yield. Participants (30 females, 9 males) either handled a 50 mL conical tube, a 250 mL glass graduated cylinder, or a wooden or plastic knife handle for 2 minutes with pressure on each hand to deposit epithelial cells. A cotton swab moistened with 100 uL of diH_2O was used to swab along the surface of the object to collect the deposited skin epithelial cells. Alternatively, a moistened cotton swab was used to directly swab the palms of the participants hands. The cotton swab was rotated while

swabbing to ensure all surfaces of the swab made contact with the cells. The swabs were lightly tweezed apart to loosen the cotton fibers for better cell elution. Swabs from each participant were placed into a single tube containing 1.5 mL of cell staining buffer (bovine calf serum, sodium azide) (BioLegend, San Diego, CA). To elute the cells from the swabs, the swabs were incubated in buffer for five minutes and then pulse agitated in a vortex platform (1 minute).

Epithelial skin cells other than from the hands were collected from participants using a Whatman® FTA® Sterile Omni Swab (GE Healthcare, Chicago, IL). Participants swabbed the sides of their nose and behind their ears for two minutes to maximize skin cell yield. Participants who were wearing makeup, or any other facial-care product, only swabbed behind their ears. Informed consent was obtained from the participants prior to collecting samples.

Antibody Staining

After the cells were eluted off of the cotton swab, the swab was discarded and the cell staining buffer containing the eluted cells was transferred to a 1.5 mL microcentrifuge tube. The cell solution was centrifuged at 14,000 Relative Centrifugal Force (RCF) for ten minutes. Without disturbing the pellet, the supernatant was removed until 250 uL remained using a P1000 micropipette; then the pellet was resuspended by pipetting up and down. One microliter of blocking buffer (aqueous buffer, proteins, 0.09% sodium azide) (Thermo Fisher Scientific, Waltham, MA) was added to the cell solution, and it was incubated on ice for ten minutes, then the cell solution was vortexed. Two new 1.5 mL microcentrifuge tubes were created to be the negative control and the isotype control. Eighty-three microliters of the cell solution were removed and placed into each new tube. The remaining 83 uL of cell solution in the original tube were not transferred to a new tube. Next, one of the cell solutions was incubated and hybridized with the FITC-labeled anti-testosterone (anti-T) antibody (Novus Biologicals, Centennial, CO)

with a concentration of 0.68 mg/mL at a volume 2.5 uL [0.0017 mg]. Another cell solution was incubated and hybridized with the FITC-labeled isotype control antibody (Novus Biologicals, Centennial, CO) with a concentration of 0.62 mg/mL at a volume of 2.5 uL [0.00155 mg]. When optimizing the antibody combination, varying volumes of anti-T [2.5 uL [0.0017 mg], 5 uL [0.0034 mg], and 10 uL [0.0068]] and anti-DHT [2.5 uL (0.001025], 5 uL [0.00205], and 10 uL [0.0041]] (MyBioSource, San Diego, CA) of antibody were added to single-source cell solutions (Table 1). The amount of antibody in mg per cell was also reported (Table 2). The remaining cell solution acted as a negative control and was not stained with any antibody or isotype antibody. All three tubes were vortexed for one minute before and after incubation on ice for one hour. Next, the cell solutions were washed in cell staining buffer. The cell solutions were centrifuged for 10 minutes at 14,000 RCF, and the supernatant was removed without disturbing the pellet until ~100 uL remained. The pellet was resuspended in 400 uL of cell staining buffer for a total volume of 500 uL. This wash was performed twice before flow cytometry analysis.

Initial evaluations of hybridization and optimizations were performed on the isotype control and anti-T antibodies with additional anti-DHT separately using flow cytometry. Hybridization was performed on both single-source cell solutions and mixture cell solutions where it was likely that each individual contributed unequal numbers of cells because individuals shed cells at different rates. For single-source samples, the unstained negative control, isotype control, and anti-T or combined anti-T and anti-DHT stained epidermal cell solutions were separately analyzed on the flow cytometer and generated fluorescence histograms to visualize the fluorescent intensities of each cell solution. This was done to evaluate whether there were noticeable differences in fluorescence between the controls and the anti-T stained samples, and which combination of anti-T and anti-DHT gave the most optimal difference in fluorescence

from the controls. The median fluorescence of the anti-T stained samples was documented for plotting against DNA quantity at a later time. For mixture samples, the fluorescence histograms of the anti-T stained samples were evaluated for the number of noticeable peaks.

Flow Cytometry Screening

Initial screening of antibody hybridization of epidermal skin cells was performed using the Guava® easyCyte™ flow cytometer. Prior to analysis on the flow cytometer, the Guava cleaning cycle and easyCheck protocol was performed. The cleaning cycle ensured that there was no particulate build up in the capillary before analyzing the epidermal skin cells. The easyCheck protocol demonstrated that the instrument counted a known number of reference beads correctly before counting the epidermal cells or events within a cell solution. Epithelial cell populations in cell staining buffer were analyzed in the Guava® easyCyte™ instrument in aliquots of 500 μL, after being passed through a 100-um filter in order to filter out components that could interfere with hybridization, which may include fragments of sampling swab and/or aggregations of cellular debris. Initial experiments used an Alexa-488 fluorescently labeled anti-T antibody, whereas later experiments used a FITC-labeled anti-T antibody. The Alexa-488 emits a higher intensity signal, but both fluorophores absorb and emit at identical spectra. The isotype control antibody and anti-DHT antibody were both FITC labeled. The epidermal skin cells bound with fluorescently labeled antibodies were moved through a capillary and individually excited with a 488 nm laser (50 mW). The anti-T stained cell solutions (222 uL) were eluted directly from the flow cytometer into a 1.5 mL DNA LoBind® low retention tube (Eppendorf, Hamburg, Germany). Cell solutions were frozen at -20°C until ready to extract DNA. After flow cytometry, the Flow Cytometry Standard (.fcs) files generated by the Guava

flow cytometer were analyzed on the FlowJo® software program (BD, Franklin Lakes, NJ). Scatter plots of the cell size (x-axis) and complexity (y-axis) were generated. Each sample was gated to contain large and complex cells and exclude potential cellular debris. Histograms of the fluorescence of each gated sample were created with the fluorescent intensity (Green-B fluorescence area log) and the cell count on the x- and y-axes, respectively.

DNA Extraction and Quantification of Cell Solutions

All cell solutions analyzed with flow cytometry were collected and subjected to DNA extraction with the DNA IQ™ System (Promega, Madison, WI) following the Virginia Department of Forensic Science's protocol (32). Purified DNA extracts were dried using the entire 40 µL using vacuum centrifugation (SpeedVac, Thermo Fisher Scientific) and re-suspended in sterile 18Ω water in 13 µL. Quantitation was performed on all purified samples with Promega's PowerQuant® System using the Quant Studio 5 Quantitative PCR instrument (AB, Foster City, CA), following the manufacturer's protocol.

Mixture Skewness vs Kurtosis Statistical Analysis

The raw fluorescence data for single-source, two-person, three-person, and four-person mixtures was exported from FlowJo (N=18). The data consisted of the individual fluorescent intensity values of each cell/event in the gate used to create the histograms for each sample. This data was exported for five of the single-source samples, two-person, and three-person mixture samples, and all three of the four-person mixture samples. A univariate analysis was performed on each sample's raw fluorescence data in the PAleontological STatistics (PAST) software to calculate the skewness and kurtosis of each sample.

The skewness of a distribution is a measure of asymmetry compared to a normal distribution, which has a skewness of zero and is completely symmetrical. A positive skewness value indicates that a distribution is skewed to the right and a negative value indicates that a distribution is skewed to the left compared to a normal distribution. The kurtosis is a measure of whether the tails of a distribution are heavy or light relative to a normal distribution. In a heavy tailed fluorescence histogram, the cell count would approach zero very slowly at the left and right tails and would have many outlier cells/events with both low and high fluorescent intensities. In a light tailed fluorescence histogram, the cell count would approach zero very quickly at the left and right tails and would have very few outlier cells/events with low and high fluorescent intensities. A kurtosis of zero means that the tails are neither heavy nor light relative to a normal distribution. A positive kurtosis value indicates a heavy-tailed distribution, and a negative value indicates a light-tailed distribution relative to a normal distribution (33). The skewness and kurtosis values for each sample were then plotted on a scatterplot. The single-source, two-, three- and four-person mixtures were color-coded to determine whether each sample type demonstrated reproducible skewness and/or kurtosis values.

Results and Discussion

Gating Data and Fluorescence Histogram Shape

The distributions of fluorescence histograms from both known single-source and mixture samples could change significantly depending on the subpopulation of cells selected for analysis. In one two-person mixture sample (Fig. 1), the histogram was consistent with as a single-source cell population with only one peak. However, as the gate was shifted to include a broader range of cells and/or other biological objects, the fluorescence histogram displayed two-distinguishable

peaks that could indicate the presence of cell populations derived from two different contributors (Fig. 1A-B). To maximize the chance of observing contributor-specific differences, one gate/subpopulation was selected based on this cell population and then applied to other cell populations generated for this study.

While some mixture samples did result in more than one distinguishable peak, it should be noted that single-source and mixture samples with a cell count at or below ~200 resulted in histograms with irregular distributions and multiple peaks that were not necessarily indicative of the number of contributors (Fig. 2A-C) (Fig. 3A-B). This could indicate that a minimum cell count is needed to make meaningful conclusions based on histogram data. It should be noted that the gating parameters used are not the most optimized, which could have impacted number of cells used to create the histogram. It is possible that a truly optimized gate could include more cells to mitigate these irregular distributions in both single source and mixture samples and still offer resolution of multiple peaks in mixture samples. Irregular histogram distributions due to low cell count were reproducible and observed three times in the same single-source donor (Fig. 2A-C) and two times in the same mixture samples (Fig. 3A-B). The same donor with a low cell count in known single-source histograms could appear to be a mixture of multiple contributors (Fig 2A-C) but was easily identifiable as a single-source sample with one peak when the cell count was larger (Fig. 2D). A known mixture of two contributors with a low cell count produced histograms that could not definitively attribute shoulders or other patterns of the histogram to multiple contributors because the low cell count could be the main factor determining the histogram shape (Fig. 3A-B). However, when the cell count was substantially greater in the known mixture of the same two contributors, there were two distinguishable peaks presented without other irregular histogram patterns (Fig. 3C). The gating parameters and the cell count

within the gate influenced the shapes of histograms, though more testing is required to determine which is more influential of the histogram shapes because changing the gating parameter also changed the number of cells within the gate that were used to create the histogram.

Isotype Control

For an individual solution of epidermal skin cells from a single donor, the fluorescence shift for an unstained control, isotype control, and anti-T stained sample were also compared on overlaid histograms to make inferences about the specificity of the anti-T antibody. In many cases the isotype control had a greater fluorescent intensity than the unstained control, while the anti-T stained cells showed a fluorescent intensity greater than both controls (Fig. 4). This demonstrates that the anti-T antibody is more specific than the isotype control because the greater fluorescent intensity of the anti-T stained cells represents a greater amount of antibody emitting a fluorescent signal, which is achieved by a higher amount of anti-T antibody binding to its target molecule(s) compared to a lower amount of isotype antibody binding. If there is a greater amount of binding and more affinity of one antibody over another, then it must be specific to a particular target molecule or molecules (34).

The anti-T antibody was identified as being more specific than the isotype control due to a greater fluorescent intensity demonstrated by a greater shift to the right (higher fluorescence) of the anti-T histogram compared to the isotype control histogram. This analysis alone does not determine that the antibody is specific to testosterone molecules within the cell, only that it is binding with higher affinity than the isotype antibody, which is known not to be specific to any

molecules within the cells, and therefore measures the amount of nonspecific binding and background fluorescence.

The median fluorescence value of the isotype control fluctuated between approximately 2,000 and 5,000 when staining single-source samples (Fig. 5). When isotype control histograms generated from four different donor's epidermal samples were overlaid, there were small differences in separation between each histogram. This indicates that between numerous, different single-source donors, the amount of nonspecific binding and background fluorescence does not vary substantially because there is limited separation between the histograms. It is possible that the differences in median fluorescence between samples are simply due to differences in cell count from sample to sample.

It should also be noted that, in some instances, the gate chosen to analyze only large and complex cells that was applied to all unstained control, isotype control, and anti-T (Fig. 6A) or anti-T and anti-DHT combined (Fig. 6B) antibody samples resulted in the complete overlap of the unstained control and the isotype control in some samples. If the fluorescent intensity of the isotype control is approximately the same as the unstained control, then it can be inferred that there was limited nonspecific binding occurring in the gated large and complex cell population; therefore, it is likely that the nonspecific binding of the isotype control predominantly occurred in the small and less complex cell population. The shift of the anti-T stained sample and the separation from the two controls demonstrates that the molecule(s) that the anti-T antibody is specific to was present in large and complex cells that likely contain more macromolecules than small and less complex cells. This can be observed in the scatterplots for these samples (Fig. 6C-D) because the gating parameter applied in figure 1A was applied to all samples including figure 7. The gate is including cells/events that have high forward scatter and high side scatter values.

Determining that the anti-T antibody was specific was important for several reasons. The amount of target molecule within the shed epidermal cells likely varies from person to person; thus, the amount of anti-T binding will likely vary from person to person and produce differing levels of fluorescence between cell populations from different donors. Therefore, it could be possible to estimate the number of contributors based on the differences in fluorescent intensity that is proportional to the amount of target molecule present in different cell populations from different donors. Because testosterone is a macromolecule, its presence could indicate the presence of other macromolecules like DNA. Since the anti-T antibody was concluded to be specific, it is possible that fluorescent intensity generated by the amount of antibody binding to a specific macromolecule could correlate to the quantity of DNA, another macromolecule, within a single sample. This was further supported by observing that the anti-T antibody was binding specifically in large and complex cells with more internal particulates, which were more likely to contain DNA.

Lastly, the greater fluorescent intensity of the anti-T antibody compared to the isotype control allowed for the anti-T antibody to be optimized with the anti-DHT antibody to produce an even greater fluorescence shift of the histogram when the same donor was stained (Fig. 7). It should be noted that the cell count of the anti-T stained sample [920 cells] of the donor was substantially higher that of the combined anti-T and anti-DHT stained sample [285 cells]. Separation was observed between the two histograms, and the median fluorescent intensities of the anti-T only [7661] and the combined anti-T and anti-DHT [22863] samples were substantially different. However, the same donor should be stained with anti-T and combined anti-T and anti-DHT again with similar cell counts in order to make a more accurate comparison between the fluorescent intensities of the overlaid histograms. It is possible that the median

fluorescent intensity of the combined antibody sample is a less accurate than the anti-T only sample because of the low cell count. One potential future direction could be to stain the hand cells with anti-T and combined anti-T and anti-DHT antibodies from many different single-source donors to determine if the combined antibody resulted in a reproducible greater shift of the histogram to the right. Only one individual donor was stained with combined anti-T and anti-DHT, so the greater shift to the right was not determined to be reproducible in this study.

Mixture Analysis

Samples Collected From "Touch" Epithelial Cell

Mixture cell solutions were created by swabbing objects that were handled by multiple participants, and subsequently eluting cells into aqueous buffer. Alternatively, single-source swabs were created after swabbing participants' palms, and cells were eluted from each swab into the same tube containing buffer to create mixtures. The fluorescence histograms were evaluated for the number of distinguishable peaks produced to assess whether or not contributor number would be reflected in the number of peaks observed in the histograms. The histograms were created using a gated subpopulation of cells that contained larger cells with forward scatter values on the x-axis between ~ 117 and ~ 263, and complex cells with side scatter values on the y-axis between ~ 2800 and ~ 93000 that was identified from the previous experiment.

It was expected that the histograms produced from the staining cell solutions containing multiple contributors could show more than one distinct number of peaks, and, possibly a number of peaks equal to the number of contributors in the cell solution if each contributor differed in the amount of testosterone targets (or other antigen recognized within the cell by the

anti-T antibody) within the population of shed skin cells. This was observed in three two-person mixtures (3/18) and one three- person mixture (1/9). However, there were many histograms generated from two-, three-, and four-person mixtures that did not show evidence of multiple peaks. Some appeared to have only one peak, similar to histograms generated from single-source cell solutions (Fig. 8).

There are many potential factors that could play a role in the lack of resolution. One major factor could be the total number of cells in the mixture belonging to each contributor. Two contributors are unlikely to shed the same number of cells after handling an object or having their hand swabbed. For example, if one contributor sheds cells more easily and donated two or three times the number of cells than a second contributor, then the first contributor could produce a histogram with a higher median fluorescence that may not be strictly due to intrinsic biochemical differences between contributor cell populations prior to shedding. One of the three-person mixtures displays two distinguishable peaks and a slight shoulder indicated by the arrow (Fig. 9). It is possible that the shoulder was the signal generated from the third contributor but could not be confidently distinguished as its own peak potentially due to low cell yield from contributor 3 relative to the other two donors. Differences in cell count would only become more prominent and difficult to mitigate as the number of contributors within a mixture increase.

The sample collection procedure itself may have been responsibe for some of the variation in donor cell contributions within the mixture. Because the cell populations from multiple donors were being eluted from different cotton swabs into the same 1.5 mL aliquot of cell staining buffer, each swab absorbed some of the cell staining buffer after the elution step resulting in loss of volume and/or cells from the mixture. This could conceivably cause

differences in donor cell populations even if contributors had originally shed roughly the same number of cells.

Another potential cause of poor resolution between cell populations could be the biochemical characteristics of the cells themselves. Skin epithelial cells are dead, highly keratinized, and often lack DNA and many other macromolecules and cell structures (2, 3, 4). While swabbing hands as a method of cell collection did result in a higher percentage of larg, er cell events, the handling of objects such as plastic conical tubes, glass graduated cylinders, and wooden or plastic knife handles often resulted in higher proportions of smaller cell events. If these smaller cell events also have fewer molecular targets, this may result in less antibody binding overall and less fluorescence differentiation across contributors.

Additionally, it is possible that two contributors donated a roughly equal number of cells that were large and complex, but the histograms still did not resolve multiple distinguishable peaks. It could be that multiple donors had comparable amounts of target molecules within their cells, so there would be roughly equal binding of the anti-T antibody in multiple donors and indistinguishable fluorescence profiles.

Finally, the gating parameters chosen were based upon one two-person mixture. It is possible that these parameters are not the most optimized parameters to apply for mixtures containing higher numbers of contributors. Future work should test a wide range of different contributors and different combinations of contributors in order to develop the most useful and reliable gating parameters for maximum distinction between contributors.

Swabbing contributors' hands directly yielded much higher cell counts including a noticeable subpopulation of large cells. Continuing with this method would mitigate any issues

in resolution due to predominantly small cell events that are likely cellular debris. A future direction to further improve resolution of contributors could involve quantifying the number of cells from single contributors after direct hand-swabbing, followed by combining the same number of cells from each contributor to create a 1:1 ratio. While this was performed previously and did not result in noticeable improvement, it should be noted that the cells were collected from plastic conical tubes which had a smaller subpopulation of large and complex cells compared to those collected from direct hand swabs. Combining the two collection methods may result in an comparable amounts of large and complex cells from each contributor, and be more optimal to resolve differences in fluorescence profiles among contributors. Elution of cells from the swabs separately into a sufficient volume and then creating the mixtures may also assist in creating representative mixtures of donors.

Samples Collected from Nose/Face Cells

In this experiment, cells were collected from the nose/face of the contributors, which shed fewer cells than the hands. This is because there are fewer layers of anucleate cells on the nose and face, and more layers of cells containing DNA and macromolecules since they are larger, more complex, and nucleated (2). Skin on the nose and face lacks the stratum lucidum, which is an additional layer of anucleate cells that exists in the hands and feet. This makes the skin of hands and feet thicker than that of the nose/face and therefore, with more cells shed from the hands and feet, but they are smaller and less complex (2). Overlaid anti-T fluorescence histograms of two different single-source contributors demonstrated that cell populations originating from different contributors could have different fluorescence signals and be differentiated from one another (Fig. 10). While there is noticeable separation each cell

population showed relatively low cell counts (272 and 257) cells, which may explain their irregular distributions. This cell collection method was discontinued in favor of the "touch" epithelial cells because the "touch" epithelial cell collection method gave higher cell yields and was more representative of "touch" evidence handled in casework when compared to nose/face cell collection method.

It should be noted that the nose/face cell histogram exhibited a greater shift to the right compared to the hand cells of the same donor when both samples were stained with anti-T probe (Fig. 11). There is a difference in fluorescent intensity between the hand and nose/face cell populations, however this may be driven in part by differences in cell counts across (644 cells and 271 cells for the hand and nose/face histograms, respectively). One potential future direction could be to stain hand and nose/face cells from many different donors and overlay the histograms to determine whether or not the greater shift to the right in nose/face cells is reproducible.

Two-Person Mixtures

The two-person mixtures (N=18) resulted in histograms with two distinguishable peaks, plateaus, single-peak distributions, as well as irregular distributions due to low cell count. Multiple mixtures displayed two distinguishable peaks in the anti-T stained samples, but also in the unstained control samples. This could indicate that there were differences between donor autofluorescence that may also be useful in estimating contributor number. Of all the two-person mixtures tested, one mixture (3/18) correctly reflected the number of contributors with two peaks in the anti-T stained samples (Fig. 12A-C). The remaining fifteen two-person mixtures only displayed one peak. Some of the mixtures displayed little to no resolution between stains with

anti-testosterone, anti-isotype and unstained control (Fig. 8B-C, Fig. 9). Whether this reflects a real phenomenon and range in staining profiles among contributors or problems with the assay itself will require further testing.

Three-Person Mixtures

The three-person mixtures (N=9) resulted in histograms with three distinguishable peaks, two distinguishable peaks, and single-peaked profiles. Of all the three-person mixtures tested, 1/9 resulted in three distinguishable peaks, and 2/9 resulted in two distinguishable peaks when stained with anti-T antibody (Fig. 13A-C). Only one mixture correctly represented the true number of contributors present by displaying three distinguishable peaks. The two mixtures that displayed two peaks did not correctly identify the exact number of contributors but were still able to predict the sample to be a mixture of at least two contributors, rather than single-source. One mixture with two peaks also displayed a slight shoulder that could be from the third contributor but was not resolved enough to clearly indicate as such. The remaining six mixtures displayed only one peak and could not identify the samples as mixtures.

Four-Person Mixtures

The four-person mixtures (N=3) resulted only in single-peaked largely symmetrical distributions. Unlike many single-source samples, there appears to be only a small separation between the isotype control and the anti-T fluorescence histograms in all of the four-person mixtures. It is possible that this minimal separation could be caused by inefficient antibody binding in the cell solution, therefore producing a relatively low fluorescent signal. It should also

be noted that consecutively eluting four different cotton swabs by agitation into a single tube of 1.5 mL of cell staining buffer resulted in a noticeable drop in cell staining buffer volume (approximately 1.0 mL) due to the absorbent nature of the swabs. Using this approach with a limited volume, it is unclear if the cells eluted from the swabs with any efficiency. This would greatly impair the ability to detect cells from each contributor if elution efficiency from each consecutive swab was impacted by the diminishing volume in which to elute the cells.

To mitigate this, the volume of the cell staining buffer could be increased to account for loss of volume during the elution of the swabs. Alternatively, the cells from each swab could be eluted into their own volumes of cell staining buffer, then the volumes could be combined to bring all cell solutions together without risking an inefficient removal of cells from the swabs. The four-person mixture histograms are not consistent with the two or three-person mixtures. Additional replicates are likely needed to assess the consistency of these results and/or if further optimizations of the method are needed.

Kurtosis vs Skewness

The skewness and kurtosis of each sample were plotted on the x- and y-axes of a scatterplot, respectively (Fig. 14). It was observed that all of the single-source samples had a positive skewness value, meaning that the histograms were all skewed to the right. The two-, three-, and four-person mixture samples displayed both positive and negative skewness values, meaning that some mixture histograms skewed to the right, while other skewed to the left. Initial observations support that samples with a positive skewness could be single-source or a mixture sample, whereas samples with a negative skewness were only mixtures. Although it did not

resolve the number of contributors, this method could potentially be a presumptive test for indicating the presence of multiple contributors based on the skewness of a fluorescence histogram.

It was also observed that all of the two- and three-person mixture samples have kurtosis values clustered around zero, whereas there is more variation in the single-source samples and four-person mixtures. Further testing for four-person mixtures is needed, given that it is unclear whether the four contributors were efficiently eluted into cell staining buffer and subsequently represented in the fluorescence histograms.

Median Fluorescent Intensity and DNA Content

The median fluorescence shift for single-source samples (N=25) was plotted against the DNA concentration or content (all DNA samples were eluted in the same volume) detected by qPCR. The scatterplot shows no correlation between the median fluorescence shift and the DNA content ($R^2 = 0.0884$) (Fig. 15). One single-source sample was excluded from the scatterplot because the autosomal DNA:*Y-chromosomal* target DNA ratio was 50.66, indicating a mixture of male and female DNA in the sample. Because the goal of this study was to measure single-source DNA, the sample was excluded. Although there was no obvious correlation between fluorescence and DNA content, it should be noted that all but two of the samples were estimated in a concentration range that showed a high percent CV (coefficient of variation) (35). The coefficient of variation measures the variability of data in a sample in relation to the mean of the data set. Since nearly all of the DNA samples were quantified at values below the limit of reliability for the PowerQuant®™ system used in conjunction with the QuantStudio 5 qPCR

instrument, no conclusions can be drawn on whether or not there is any correlation between fluorescence shift and DNA content.

Although there was no discernable correlation between fluorescence intensity and DNA content, one observation may still support the hypothesis. The median fluorescence for single-source samples increased as the gating settings are changed to include only large and complex cellular events, whereas the fluorescence decreased when small and simple events were included in the gate (Fig. 16A-C). There is a greater chance that cells will contain DNA if they are characterized as having larger FSC and SSC profiles. Because there was a greater fluorescence shift to the right as more large and complex cells were included in the gate, it appeared that the anti-T antibody was binding to its target molecules more efficiently in large and complex cells. Therefore, more antibody binding resulting in a greater fluorescence shift may still be correlated to DNA content. To confirm this, there would need to be enough DNA present within the touch epithelial samples to be above the limit of reliable quantitation to accurately correlate fluorescence and DNA content. In order to improve DNA yield, cell solutions to undergo DNA extraction were collected and stored in low retention tubes so that released DNA was not lost due to binding to the collection tube itself. In addition to this, future improvements may include low retention pipette tips to further prevent DNA loss due to binding and more effective DNA extraction techniques for low template samples.

Anti-T and Anti-DHT Antibody Optimization

The total amounts of anti-T and anti-DHT antibodies were varied when staining cells in order to determine which combination of antibodies would yield the most optimal fluorescence

shift from the unstained and isotype controls. Given that ~10% of testosterone in target tissues is converted to dihydrotestosterone, it is conceivable that the hormone staining signal could be amplified by staining cells with both antibodies simultaneously. Multiple skin epithelial touch samples were obtained from the same donor, and each sample was stained with a different amount of anti-T and anti-DHT antibodies. The same donor was used for all combinations. The same donor was used to control for the possibility of differences in fluorescence shift due to differences in antibody binding between to different donors rather than the amount of antibody used. Most samples that were stained with 0.0034 mg [5 uL] or 0.0068 mg [10 uL] of anti-T antibody, regardless of the amount of anti-DHT antibody present, exhibited a noticeable upward tail at the rightmost end of the x-axis (Fig. 17A, 17C, 18A-C). It is possible that this was an artifact that occurred due to a large amount of fluorescence generated from excess antibody in the sample that was not bound to any target molecules; the artifact could be indicative that the cell solution was oversaturated with antibodies. Another potential factor to produce this artifact could be the clumping of many hybridized cells together during flow cytometry that were counted as one highly fluorescent cell/event. If the cell/event were included in the gate to make the fluorescence histogram, it could have potentially caused a dramatic change in the histogram shape by counting one event with a much greater fluorescent intensity than the other cells/events.

Some of the histograms generated displayed one peak as expected because the staining was performed on a single-source donor, however other histograms displayed multiple peaks that could be misinterpreted as a two-person mixture if the sample were not already known to be a single-source donor. The histograms displaying two peaks all had relatively low cell counts below or only slightly above 200, which could be a factor contributing to the multiple peaks. It is also possible that the shift in specific staining and appearance of one or two peaks may also be

affected by the different antibody mixtures used to stain cells, though further testing would be required.

The sample stained with 0.0017 mg of anti-T and 0.001025 mg of anti-DHT (3.288E-6 mg anti-T/cell, 1.983E-6 mg anti-DHT/cell) yielded the highest median fluorescence of 23915, but also exhibited a tail similar to the samples stained with larger total amounts of anti-T (Fig. 19A). The other two samples stained with 0.0017 mg of anti-T and either 0.00205 mg or 0.0041 mg of anti-DHT (7.083E-6 mg anti-T/cell and 8.542E-6 mg anti-DHT/cell or 5.965E-6 mg anti-T/cell and 1.439E-5 mg anti-DHT/cell) did not exhibit tails (Fig. 19B-C). The 5.965E-6 mg anti-T/cell and 1.439E-5 mg anti-DHT/cell sample has the greatest separation from the unstained and isotype controls. However, it should be noted that the fluorescence shift in the two controls for this sample were less than those of the other two samples stained with 0.0017 mg of anti-T. Therefore, the greater separation between the anti-T and anti-DHT histogram and the control histograms may not be due to an increase in fluorescence shift in the anti-T and anti-DHT histogram, but a lesser fluorescence shift in the control histograms compared to other samples. The isotype controls from the three samples stained with 0.0017 mg anti-T were overlaid on a histogram to demonstrate the differences in their shifts (Fig. 20A). It should be noted that the cell counts of these isotype control histograms were only slightly above 200 or even below 200 cells [378, 181, 232 cells] and are likely a factor contributing to the multiple peaks observed in the histograms, even though they are from the same known single-source donor. The samples stained with 0.0017 mg of anti-T antibody and varying amounts of anti-DHT (0.001025 mg, 0.00205 mg, and 0.0041 mg) all produced fluorescence histograms that greatly overlapped and median fluorescent intensities of 23915, 23186, and 22863, respectively (Fig. 20B).

The optimal combination of anti-T and anti-DHT antibody was one of the following combinations of anti-T and anti-DHT: 3.288E-6 mg anti-T/cell and 1.983E-6 mg anti-DHT/cell, 7.083E-6 mg anti-T/cell and 8.542E-6 mg anti-DHT/cell, or 5.965E-6 mg anti-T/cell and 1.439E-5 mg anti-DHT/cell. More specific conclusions could not be drawn due to the tail observed in the 3.288E-6 mg anti-T/cell and 1.983E-6 mg anti-DHT/cell histogram that may demonstrate oversaturation, while the samples with greater amounts of anti-DHT do not display this artifact. This experiment could be repeated using only 0.0017 mg anti-T and variable amounts of anti-DHT to determine whether the tail is reproducible in the 0.001025 mg anti-DHT sample. If the artifact was an anomaly in this experiment, then 0.0017 mg anti-T and 0.001025 mg anti-DHT [3.288E-6 mg anti-T/cell and 1.983E-6 mg anti-DHT/cell] would be most likely be the optimal combination because it yields a similar fluorescence shift to the others with less antibody.

It was observed that the median fluorescent intensity of the combined 2.5 uL anti-T and 10 uL anti-DHT histogram [22863] was substantially greater than the median fluorescent intensity of the same donor stained with only anti-T histogram [7661] when the two histograms were overlaid. However, because the cell count of the only anti-T stained sample [920 cells] was much greater than the combined 2.5 uL anti-T and 10 uL anti-DHT sample [285 cells], the amount of true separation of the histograms was difficult to accurately conclude. A future study could include comparing both staining patterns from the same donor with similar cell counts to confirm whether there is a substantial separation of the histograms. Furthermore, multiple donors could be tested to determine whether an observed separation is reproducible.

It should also be noted that some of the anti-T and anti-DHT histograms display multiple peaks (Fig. 18A, 18C, and 19B), even though the same known single-source donor was used for

all histograms. It is likely that the multiple peaks could be due to a low cell count near 200 cells, because the cell counts for the three histograms with multiple peaks (Fig. 18A, 18C, and 19B) were, 216, 322, and 240 cells, respectively. This has been observed in other known single-source samples with cell counts near or below 200 cells.

No conclusion could be drawn as to which amount of anti-DHT antibody is optimal in combination with 0.0017 mg of anti-T because the tail artifact at the upper limit of fluorescence in the histograms that appears to be associated with the oversaturation of antibody is observed in the sample stained with the smallest amount of anti-DHT antibody [0.001025 mg], but not in the larger amounts [0.00205 mg and 0.0041 mg]. In order to understand more about the causes of this artifact, this experiment should be repeated on multiple and different single-source contributors to ensure that consistent and reproducible results can be obtained regarding the level of separation from the controls, as well as the frequency of the tail artifact.

One potential future direction would be to repeat the isotype control experiments using anti-DHT as the test antibody to determine whether it is specific. This would provide further insight to the optimized combination of the anti-T and anti-DHT antibodies by determining whether anti-DHT contributes to further greater of the histogram by binding to target molecules or only by adding nonspecific fluorescence. This could allow for future directions such as staining mixture samples with both antibodies to obtain potentially gain more resolution of multiple contributors.

Conclusions

There was consistent and reproducible separation and increased fluorescent intensity of the anti-T histograms when compared to the unstained control and isotype control histograms. This was true for both single-source and mixture samples, which indicates increased binding and fluorescence compared to the measure of background fluorescence of the isotype control. This indicates that the anti-T antibody is specific, which laid the groundwork for the testing of mixtures, correlation tests of fluorescence and DNA content, as well as optimizing the antibody with the anti-DHT antibody. A previous study had demonstrated that anti-T stained cells showed a reproducible shift in fluorescence from the unstained control and that was also observed in this study (28). Frequently, the unstained and isotype control histograms completely overlapped, but it was also observed that there was a slight shift in fluorescence for the isotype control versus the unstained.

Multiple peaks within the anti-T histograms were observed in many of the two- and three-person mixtures, although the four-person mixtures only displayed one distinguishable peak. There may be many factors that contribute to the lack of resolution of the number of contributors such as imbalances in cell yield from each contributor, poor cell quality including too few large cells with macromolecules and/or internal particulate complexity, similar amounts of target molecules in multiple contributors, and inadequate removal of cells from the swabs, with particular impact on mixture samples, due to the methodology employed. Potential ways to mitigate these issues could be the collection of cells from each donor in separate eluent volumes, then mixing the volumes together and reducing the volume prior to antibody staining.

Because mixtures of touch DNA are common in the field of forensics, an orthogonal method to STR profile interpretation that nondestructively estimates the number of contributors in epithelial cell “touch” samples is a promising avenue for further studies. This method has the

potential to become a preliminary test for the number of contributors in a DNA mixture and may save time and resources by determining whether a mixture has too many contributors and too little DNA to justify downstream STR profile interpretation. Moreover, knowledge that the touch evidence consists of a mixture may assist in DNA profile interpretation.

An additional presumptive test for nondestructively indicating the presence of a mixture could be calculating the skewness and kurtosis of an epidermal "touch" sample. Because all single-source samples had a positive skewness value, it could be a possible indicator for the presence of a mixture by identifying negative skewness values. Still, both single-source and mixture samples had positive skewness values, too, so a positive skewness value may not indicate whether a sample is single-source, or a mixture based on the results of this study. Further testing is required to develop stronger conclusions. Many two- and three-person mixtures had a kurtosis value close to zero, while single-source and four-person mixture samples had more variation. Near-zero kurtosis values could be another indicator of mixtures, though the experiment must be repeated with more samples and more confidence that the four-person mixtures are being created and represented efficiently without potentially losing contributors.

There was no correlation observed between the median fluorescent intensity and the DNA content of single-source samples when plotted on a scatterplot. No final conclusions could be drawn on the relationship because the quantified DNA of most single-source samples was below the limit of reliability for the PowerQuant System used in conjunction with the QuantStudio 5 qPCR instrument, according to internal validation at VDFS. However, the median fluorescent intensity did appear to increase as the gate was continuously moved to contain only larger cells. The larger cells are more likely to contain macromolecules such as

testosterone and DNA, so the increase in fluorescent intensity supports the hypothesis that there could be a correlation between fluorescence and DNA content.

It may still be possible to observe a correlation if the amount of DNA detected was above the limit of reliability. The use of low retention pipette tips in addition to the low retention microcentrifuge tubes and possibly a DNA purification method that was superior to that used for low template DNA may provide higher yields. Moreover, it has been reported that STR profiling of DNA may be a more reliable means of estimating DNA quantity for low template samples, so this may provide a more accurate means of template yield comparison (36). If successful, this non-destructive method could serve as a preliminary estimation of the quantity of DNA within a touch sample and could save resources and time in crime labs if the estimation is deemed too low to warrant DNA quantification and STR profiling.

Most of the tested combinations of anti-T and anti-DHT antibodies in which the amount of anti-T antibody was 6.039E-6 mg/cell or higher produced a tail artifact at the upper limit of fluorescence on the histogram. It is possible that this artifact was a result of antibody oversaturation because excess antibody will bind with low affinity and increase background fluorescence that could result in lower resolution (37, 38). Another possible cause for the tails could be that multiple stained cells clumped together and were analyzed as one cell/event, resulting in a much greater fluorescent intensity relative to the other cells/events collected. If this cell/event were included in the gate, it could have skewed the fluorescence histogram to the right and resulted in a tail artifact. The optimal combination of both antibodies could not be determined beyond 0.0017 mg of anti-T and some variable amount of anti-DHT. This is because the tail artifact was observed when the lowest amount of anti-DHT was present (Fig. 19A) but not observed in the higher amounts of anti-DHT (Fig. 19B-C). It should be noted that this

observed tail was small compared to the other tails observed in other anti-T and anti-DHT combinations. It is possible that this tail is related to a factor other than antibody oversaturation like the clumping of cells stained with antibody during cell counting on the flow cytometer. The possibility that the tail could be unrelated to antibody oversaturation is supported because no tails were observed in samples stained with 0.0017 mg anti-T and the greater amounts of anti-DHT antibody (Fig. 19B-C). The median fluorescence values for all three samples were approximately the same and the histograms all showed a large amount of overlap (Fig. 20B). In order to determine a single, optimal combination, the experiment should be repeated using various single-source contributors to ensure reproducibility and assess how common the tail artifact is in samples stained with 0.0017 mg of anti-T and different quantities of anti-DHT antibodies.

One last possible future direction could be to repeat many of these experiments using cells collected from participants' noses and from behind the ears because these cells tend to be larger, more complex, and contain more macromolecules like testosterone and DNA. One prominent disadvantage to this direction is that the cells from an individual's face are not as related to evidence samples encountered in casework. Though the cells are not technically "touch" samples, it is difficult to accurately simulate casework since most "touch" items of evidence have been handled repeatedly, with pressure, frequently under condition of duress (such as an armed robbery) where sweating occurred and thus, often a greater amount of material is deposited than what can be simulated in the laboratory. Collecting epidermal cells that contain more macromolecules could serve as a means of further proving the concepts outlined in this study. Performing studies on nose/face cells may act as a substitute for the difference in the quality of the cell populations between true casework evidence and the simulated touch samples.

References

1. Kanokwongnuwut, P., Kirkbride, L. P., & Linacre. A. (2018). Detection of latent DNA. Forensic Science International: Genetics, 37(1), 95-101.
2. Betts, J. G., Desaix, P., Johnson E. Johnson, J. E., Korol, O., Kruse, D., Poe, D., et al (2013). *Anatomy and Physiology*. OpenStax.
3. (Koster, M., I. (2009). Making an Epidermis. *International Symposium on Olfaction and Taste*, 1170(1), 7-10.
4. Nakamura, K., Ito, Y., Matsumoto, K., Daikoku, E., Kiyokane, K., & Otsuki, Y. (1999). The Relationship between Apoptosis and Keratinization in Human Epidermis. Acta Histochemica Et Cytochemica, 32(1), 77–83.
5. Vandewoestyne, M., Van Hoofstat, D., Franssen A, et al. (2013). Presence and potential of cell free DNA in different types of forensic samples. Forensic Science International: Genetics. 7(2): 316– 20. 32
6. Stanciu, C. E., Philpott, M. K., Kwon, Y. J., Bustamante, E. E., & Ehrhardt, C. J. (2015). Optical characterization of epidermal cells and their relationship to DNA recovery from touch samples. F1000Research, 4, 1360.
7. Butler, J. M. (2011). *Advanced topics in forensic DNA typing: Methodology.* Elsevier Science & Technology.
8. Van Oorschot, R. A., Ballantyne, K. N., & Mitchell, R. J. (2010). Forensic trace DNA: a review. Investigative genetics, 1(1), 14.
9. Morling, N., Bastisch, I., Gill, P., & Schneider, P. M. (2007). Interpretation of DNA mixtures – European consensus on principles, Forensic Science International Genetics, 1(3-4), 291-292.

10. Suttipasit, P. (2019). Forensic Spermatozoa Detection. The American Journal of Forensic Medicine and Pathology, 40(4), 304–311.
11. Promega Corporation. (2021). PowerQuant® system technical manual. https://www.promega.com/-/media/files/resources/protocols/technical-manuals/101/powerquant-system-technical-manual.pdf?la=en
12. Applied Biosystems. (2018). Quantifiler HP and Trio DNA Quantification Kits User Guide. https://assets.thermofisher.com/TFS-Assets/LSG/manuals/4485354.pdf
13. Butler, J. M. (2014). *Advanced topics in forensic DNA typing: Interpretation*. Elsevier Science & Technology.
14. Word, C.J. (2011). Mixture Interpretation: Why is it Sometimes So Hard? Promega Corporation website. Available from: https://www.promega.com/resources/profiles-in-dna/2011/mixture-interpretation-why-is-it-sometimes-so-hard/
15. Bieber, F. R., Buckleton, J. S., Budowle, B., Butler, J. M., & Coble, M. D. (2016). Evaluation of forensic DNA mixture evidence: Protocol for evaluation, interpretation, and statistical calculations using the combined probability of inclusion. BMC Genetics 17, 125.
16. Ladd, C., Lee, H. C., Yang, N., & Bieber, F. R. (2001). Interpretation of complex forensic DNA mixtures. Croatian Medical Journal, 42(3), 244-246.
17. Gill, P., Curran, J., Neumann, C. (2008). Interpretation of complex DNA profiles using Tippett plots. Forensic Science International: Genetics Supplement Series I, 646-648.
18. Gill, P., Haned, H., Bleka, O., Hansson, O., Dørum, G., & Egeland, T. (2015). Genotyping and interpretation of STR-DNA: Low-template, mixtures and database

matches – Twenty years of research and development. Forensic Science International: Genetics, 18, 100-117.

19. De Gendt, K., & Verhoeven, G. (2012). Tissue- and cell-specific functions of the androgen receptor revealed through the conditional knockout models in mice. Molecular and Cellular Endocrinology, 352(1-2), 13-25.
20. Marchetti, P. M., & Barth, J. H. (2013). Clinical biochemistry of dihydrotestosterone. Annals of Clinical Biochemistry, 50(2), 95–107.
21. Gottlieb, B., Lombroso, R., Beital, L. K., Trifiro, M. A. (2004). Molecular pathology of the androgen receptor in male (in)fertility. Reproductive BioMedicine Online, 10(1): 42-48.
22. Atkins, P. W. *Molecules*. (1987). New York: W. H. Freeman.
23. Hoberman, J. M., Yesalis, C. E. (1995). The History of Synthetic Testosterone. Scientific American, 272, 76–82
24. Handelsman, D. J. (2020). Androgen physiology, pharmacology, use and misuse. MDtext.com, Inc.
25. Grino, P.B., Griffin, J.E., & Wilson, J.D. (1990). Testosterone at high concentrations interacts with the human androgen receptor similarly to dihydrotestosterone. Endocrinology. 126(2),1165–1172.
26. Zouboulis, C.C., Chen, W.C., Thornton, M.J., Qin, K., Rosenfield, R. (2007). Sexual hormones in human skin. Hormone and Metabolic Research. 39(2), 85–95.
27. Stroud, L.R., Solomon, C., Shenassa, E., Papandonatos, G., Niaura, R., Lipsitt, LP. et al. (2007). Longterm stability of maternal prenatal steroid hormones from the

National Collaborative Perinatal Project: still valid after all these years. Psychoneuroendocrinology. 32(2), 140–150.

28. Miller, J. M., Brocato, E. R., Yadavalli, V. K., Greenspoon, S. A., & Ehrhardt, C. J. (2019). Testing hormone-specific probes for presumptive detection and separation of contributor cell populations in trace DNA mixtures. BioRxiv.
29. Valeggia, C., & Nũnez de-la Mora, A. (2015). Human Reproductive Ecology, 295-308.
30. Weisz, J., & Ward, I., L. (1980). Plasma testosterone and progesterone titers of pregnant tats, their male and female fetuses, and neonatal offspring. Endocrinology, 106, 306- 316.
31. Krishan, A., Krishnamurthy, H, & Totey, S. (2010). *Applications of flow cytometry in stem cell research and tissue regeneration.* John Wiley & Sons, Inc.
32. Virginia Department of Forensic Science Forensic Biology Procedures Manual, Extraction of DNA. https://www.dfs.virginia.gov/wp-content/uploads/2020/07/210-D2004-FB-PM-Extraction-of-DNA.pdf date of attainment: 5/4/2021
33. Cain, M. K, Zhang, Z., & Yuan, K. (2017). Univariate and multivariate skewness and kurtosis for measuring nonnormality: Prevalence, influence and estimation. Behavior Research Methods, 1716-1735.
34. Janeway, C.A. Jr, Travers, P., Walport, M., et al. (2001). The interaction of the antibody molecule with specific antigen. *Immunobiology: The immune system in health and disease. 5th edition.* New York: Garland Science.
35. Virginia Department of Forensic Science. (2020). Validation of the Quant Studio 5 System Draft v.6

36. Klavens, A., Kollmann, D. D., Elkins, K. M., & Zeller, C. B. (2020). Comparison of DNA yield and STR profiles from the diaphysis, mid-diaphysis, and metaphysis regions of femur and tibia long bones. Journal of Forensic Sciences, 66, 1104-1113.
37. Bio-Rad Laboratories, Inc. Antibody titration in flow cytometry. https://www.bio-rad-antibodies.com/flow-antibody-titration.html date of attainment 5/4/2021
38. Kalina, T., Lundsten, K., & Engel, P. (2019). Relevance of antibody validation in flow cytometry. Journal of Qualitative Cell Science, 97A, 126-136.

Critical Data: Tables

Table 1. All anti-testosterone and anti-dihydrotestosterone antibody volume combinations for the antibody optimization study.

		Anti-dihydrotestosterone		
	Anti-T uL, anti-DHT uL	2.5 uL (0.001025 mg)	5 uL (0.00205 mg)	10 uL (0.0041 mg)
Anti-testosterone	2.5 uL (0.0017 mg)	2.5 uL, 2.5 uL	2.5 uL, 5 uL	2.5 uL, 10 uL
	5 uL (0.0034 mg)	5 uL, 2.5 uL	5 uL, 5 uL	5 uL, 10 uL
	10 uL (0.0068 mg)	10 uL, 2.5 uL	10 uL, 5 uL	10 uL, 10 uL

Table 2. All anti-testosterone and anti-dihydrotestosterone antibody volume combinations expressed in mg/cell for the antibody optimization study.

		Anti-dihydrotestosterone		
	Anti-T mg/cell Anti-DHT mg/cell	2.5 uL (0.001025 mg)	5 uL (0.00205 mg)	10 uL (0.0041 mg)
Anti-testosterone	2.5 uL (0.0017 mg)	3.288E-6 mg/cell, 1.983E-6 mg/cell	7.083E-6 mg/cell 8.542E-6 mg/cell	5.965E-6 mg/cell 1.439E-5 mg/cell
	5 uL (0.0034 mg)	6.039E-6 mg/cell 1.821E-6 mg/cell	1.753E-5 mg/cell 1.057E-5 mg/cell	1.441E-5 mg/cell 1.737E-5 mg/cell
	10 uL (0.0068 mg)	3.148E-5 mg/cell 4.745E-6 mg/cell	2.753E-5 mg/cell 8.300E-6 mg/cell	2.112E-5 mg/cell 1.273E-5 mg/cell

Critical Data: Figures

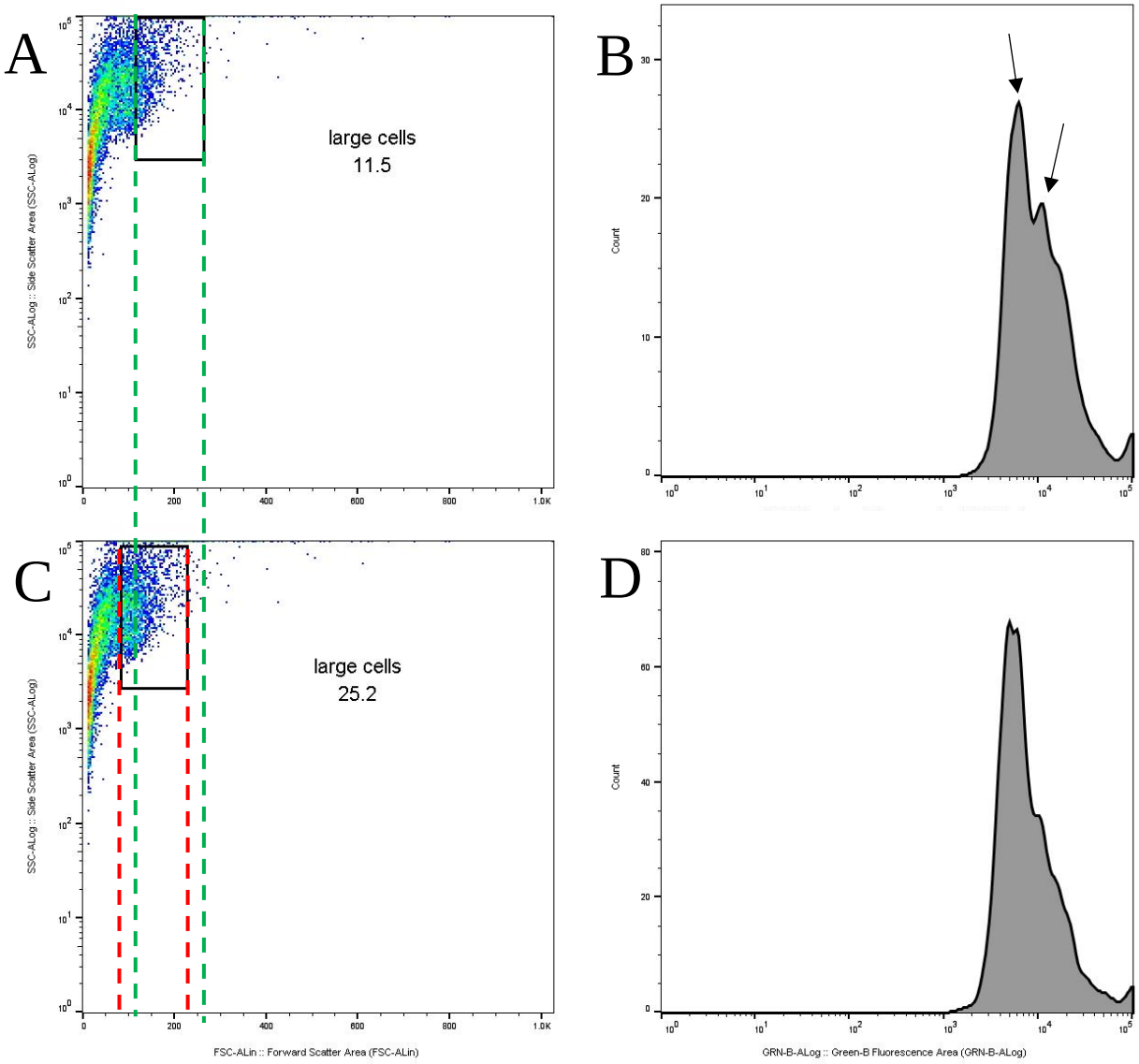

Figure 1. A known two-person mixture. **A.)** The scatterplot of cells/events with a gate shifted to the right to include large and more complex cells. The dotted green line is shown for comparison to the gate in C. **B.)** The fluorescence histogram generated from the gate on the scatterplot in A displaying two distinguishable peaks. **C.)** The scatterplot of cells/events shifted to the left to include small and less complex cells or cell debris. The dotted red line is shown for comparison to the gate in A. **D.)** The fluorescence histogram generated from the gate on the scatterplot in C displaying only one peak.

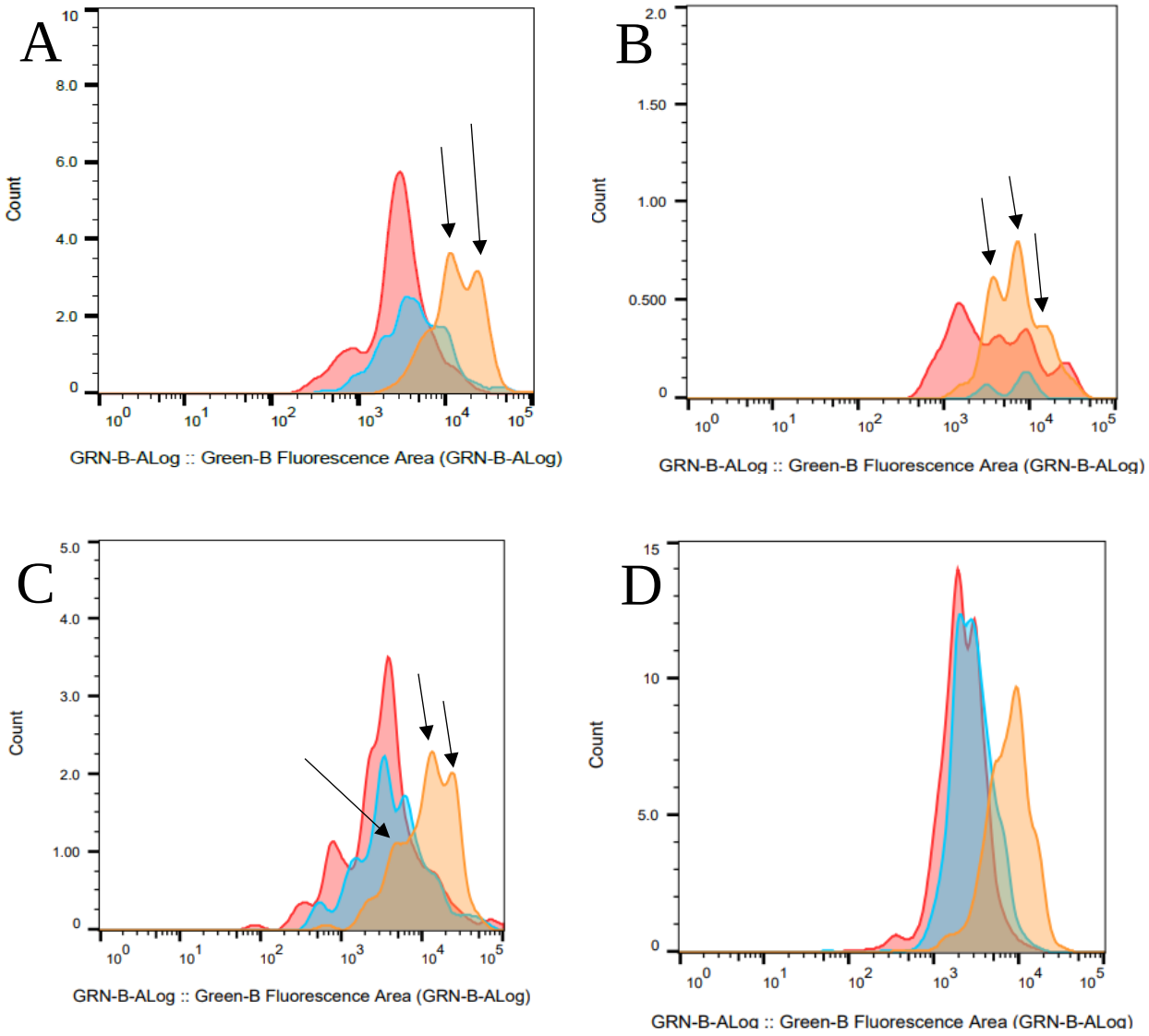

Figure 2 (A-D). Unstained (red), isotype (blue), and anti-testosterone (orange). The same single-source donor was used for A, B, C, and D. All three histograms in figures 3A and 3B had a relatively low cell count below 200 cells. The histograms in 3C all had a cell count above 200 cells **A.)** Anti-testosterone histogram cell count: 133 cells. The known single-source sample appears as if it is a two-person mixture because it displays two distinguishable peaks indicated by the arrows. **B.)**. Anti-testosterone histogram cell count: 28 cells. Samples appears as if it is at least a two-person mixture, or it could be mistaken as a three-person mixture due to the two distinguishable peaks and the shoulder, all indicated by the arrows. **C.)** Anti-testosterone histogram cell count: 95 cells. Exhibits a similar pattern to B. **D.)** Anti-testosterone histogram cell count: 298 cells. The increase in cell count has demonstrated a single peak that could not be mistaken as a mixture.

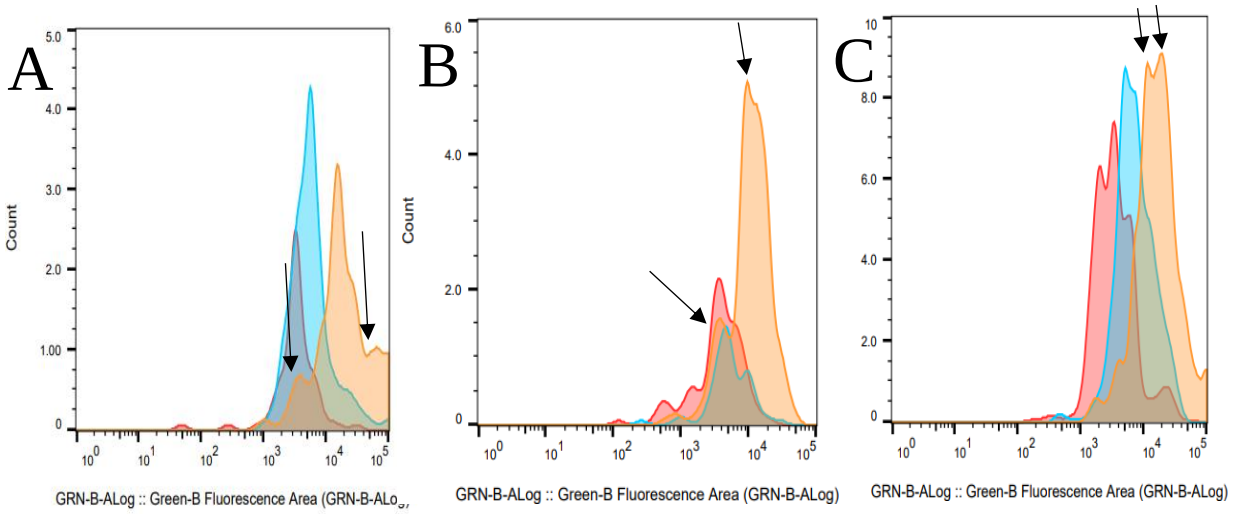

Figure 3 (A-C). The same two contributors were used to create the two-person mixtures in A, B, and C. **A.)** Anti-testosterone histogram cell count: 119 cells. The known mixture displays small shoulders in the histogram indicated by the arrows, but neither can definitively be attributed to a second contributor due to the unreliable staining patterns of low cell count samples. **B.)** Anti-testosterone histogram cell count: 173 cells. Exhibits a similar pattern to A**. C)** Anti-testosterone histogram cell count: 368 cells. The mixture displays two distinguishable peaks in the histogram that are more easily attributable to the two contributors because the distribution is much smoother compared to A.

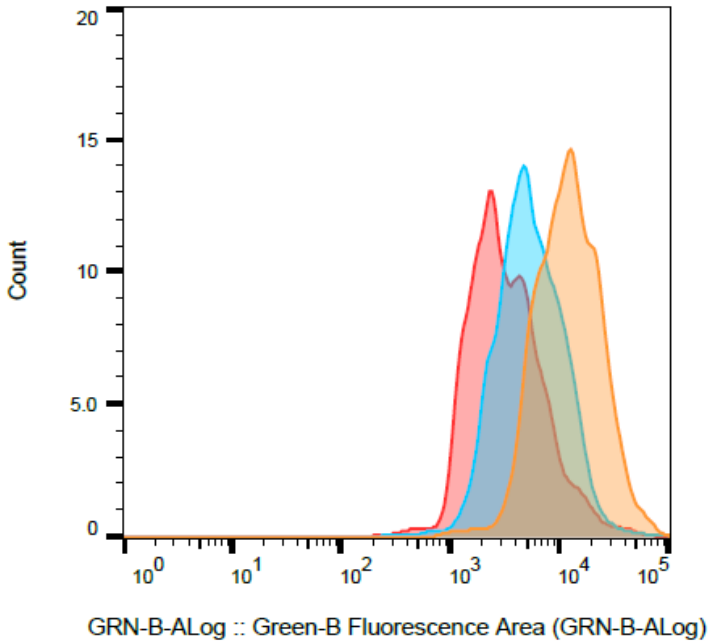

Figure 4. Unstained (red), isotype control (blue), and anti-Testosterone (orange) for a single-source contributor.

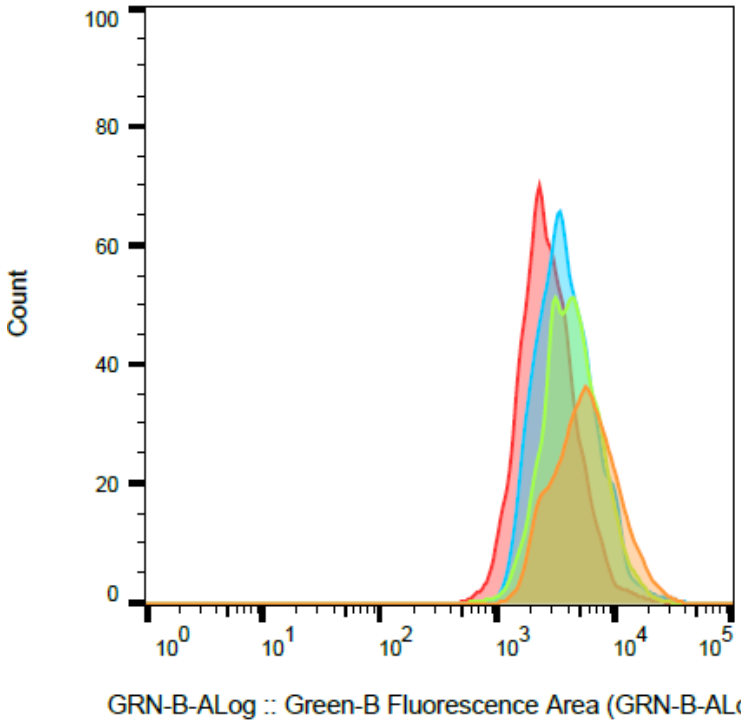

Figure 5. Four different contributors all stained with the isotype antibody showing a great amount of overlap. Median fluorescence values. Red = 2581; Blue = 3617; Green = 4222; Orange = 5623

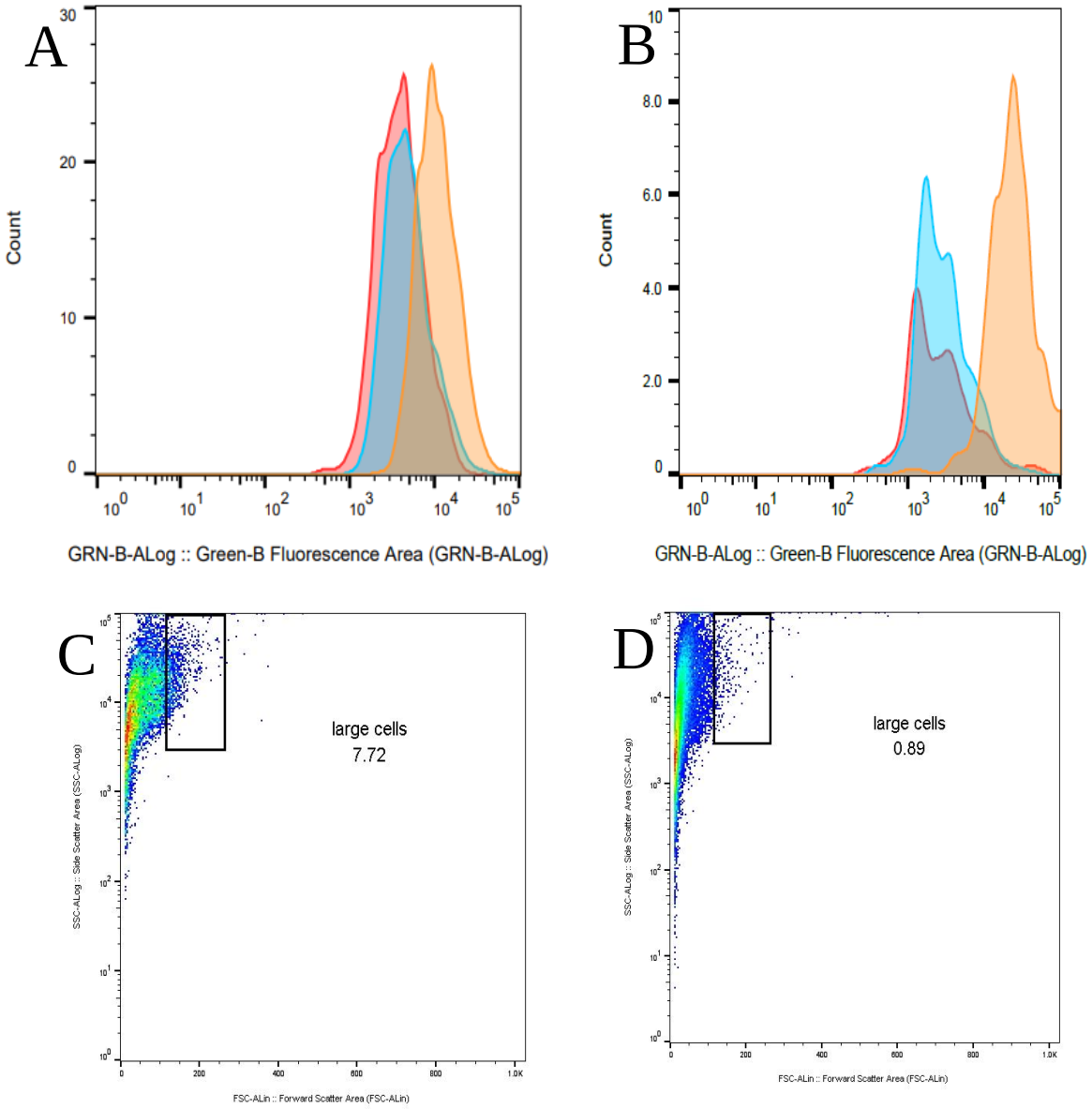

Figure 6 (A-D). The same single-source donor used for each histogram. Unstained control (red), and isotype control (blue) have a very large overlap when gating for only large cells. **A.)** Anti-testosterone (orange). Anti-T histogram median fluorescence = 10090. **B.)** Unstained (red), isotype (blue), and anti-testosterone combined with anti-DHT (orange). Anti-T+anti-DHT median fluorescence = 22863. **C.)** Scatter-plot and gate containing the cells/events used to create the anti-T histogram in A. **D.)** Scatter-plot and gate containing the cells/events used to create the combined anti-T and anti-DHT histogram in B.

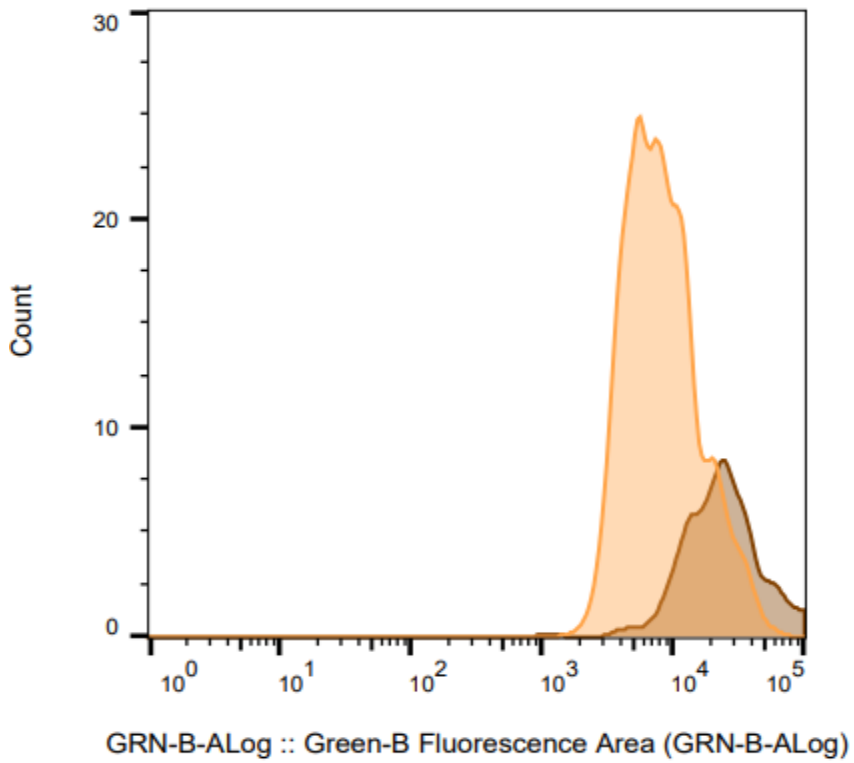

Figure 7. Epidermal cells from the palm of the hand stained with anti-T (light orange), and epidermal cells stained with 2.5 uL anti-T and 10 uL anti-DHT (dark orange) histograms overlaid. The same donor was used for both samples. The combined anti-T and anti-DHT histogram appears to have a greater fluorescent intensity compared to the anti-T only histogram, though there is a large difference in cell counts between the two samples, and a better comparison between the fluorescent intensity for the different cell types would be made with similar cell counts. Anti-T only cell count = 920 cells; median fluorescence = 7661. Anti-T and anti-DHT cell count = 285 cells; median fluorescence = 22863.

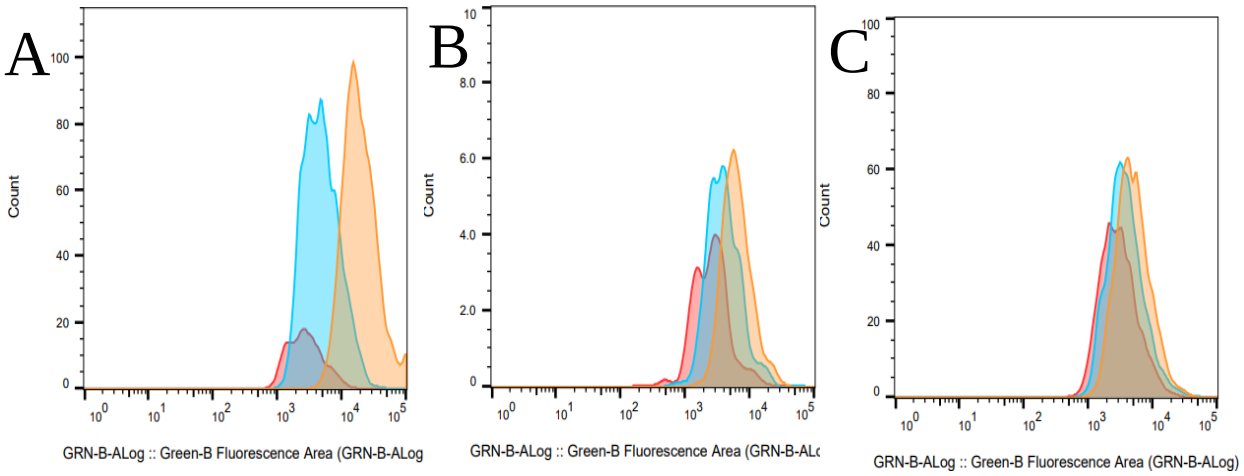

Figure 8 (A-C). Uninformative mixture histograms displaying only one peak. **A.)** Two-person mixture. **B.)** Three-person mixture. **C.)** Four-person mixture.

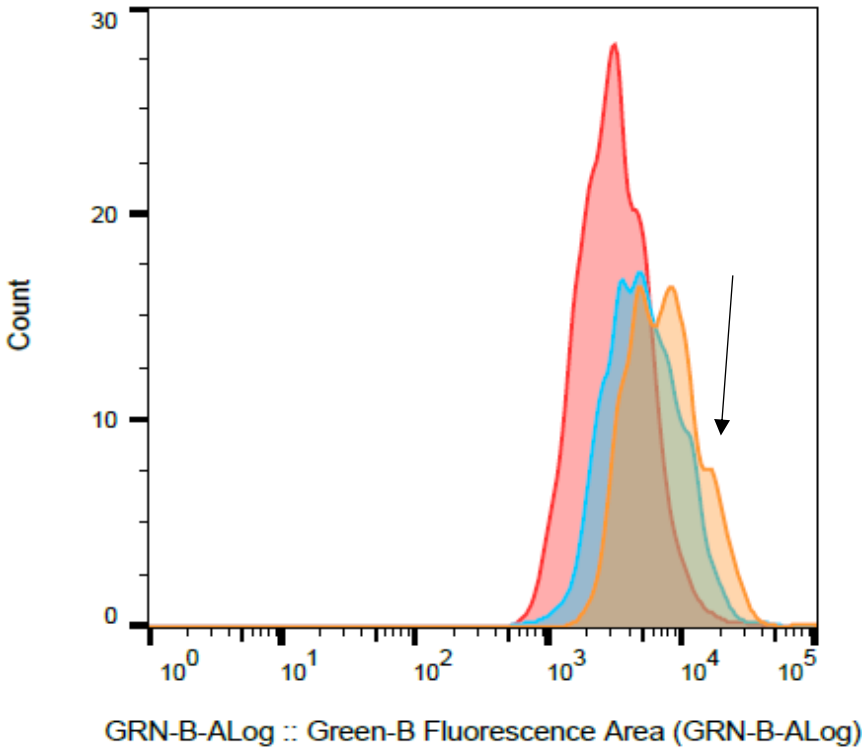

Figure 9. Three-person mixture. Two distinguishable peaks and one shoulder indicated by the arrow. Possible third donor with lower cell yield.

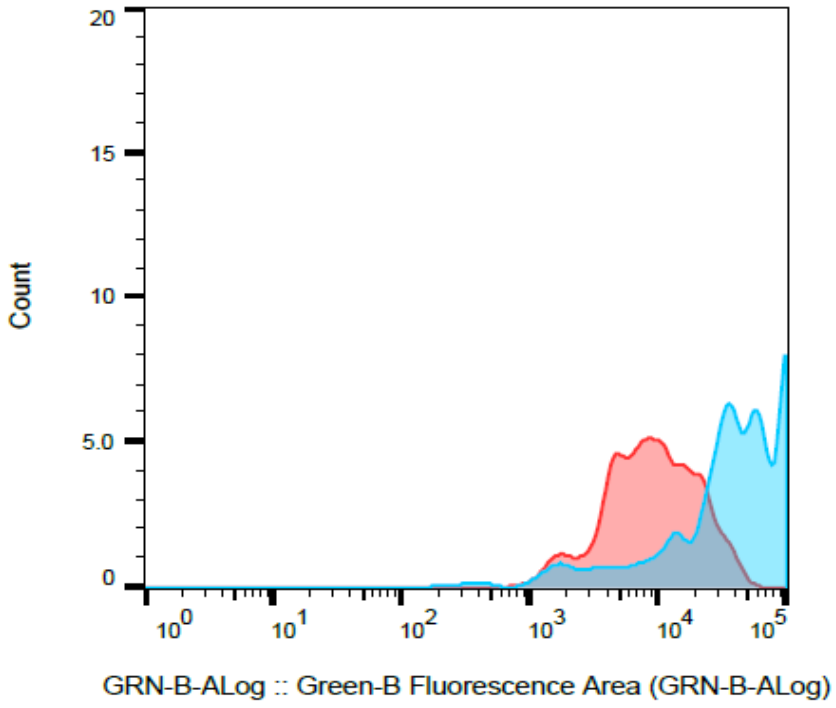

Figure 10. Nose/face cells from donor 1 (red) and donor 2 (blue) overlaid histogram. Blue cell count: 272; red cell count: 257.

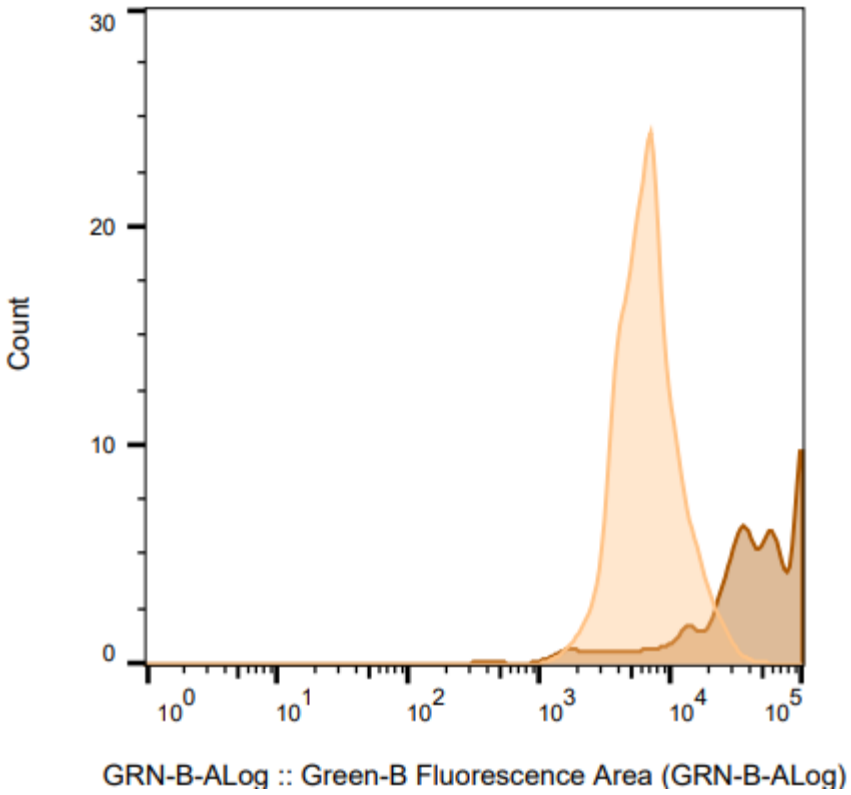

Figure 11. Epidermal cells from the palm of the hand (light orange) stained with anti-T, and epidermal nose/face cells (dark orange) stained with anti-T histograms overlaid. The same donor was used for both samples. The nose/face cells appear to have a much greater fluorescent intensity compared to the hand cells, though there is a large difference in cell counts between the two samples, and a better comparison between the fluorescent intensity for the different cell types would be made with similar cell counts. Hand cells count = 644 cells. Nose/face cells = 271 cells.

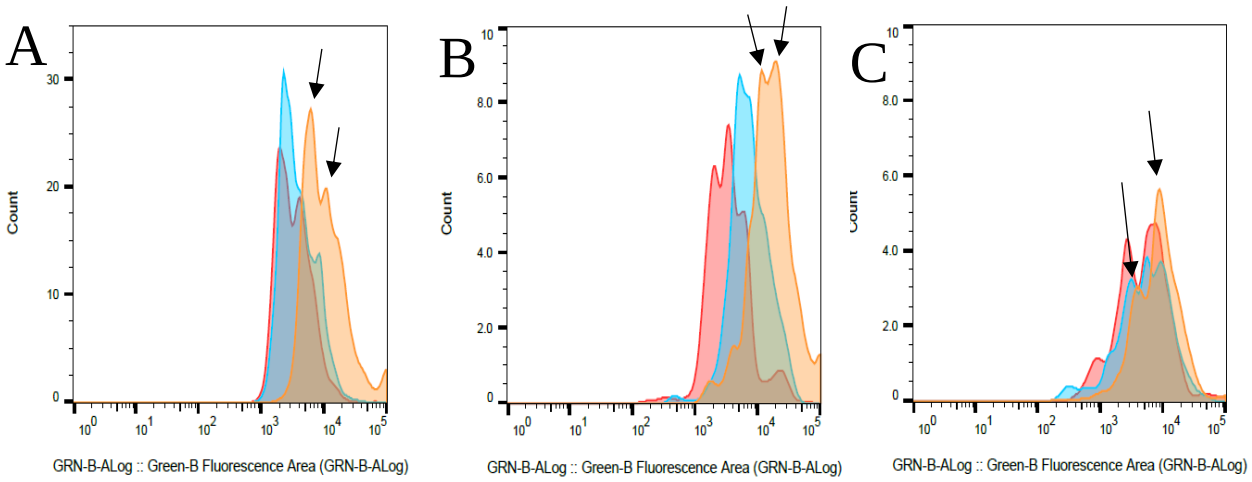

Figure 12 (A-C). Two-person mixtures with two distinguishable peaks. Unstained (red), isotype (blue), and anti-testosterone samples (orange). Each of the two peaks in the anti-testosterone are indicated by arrows.

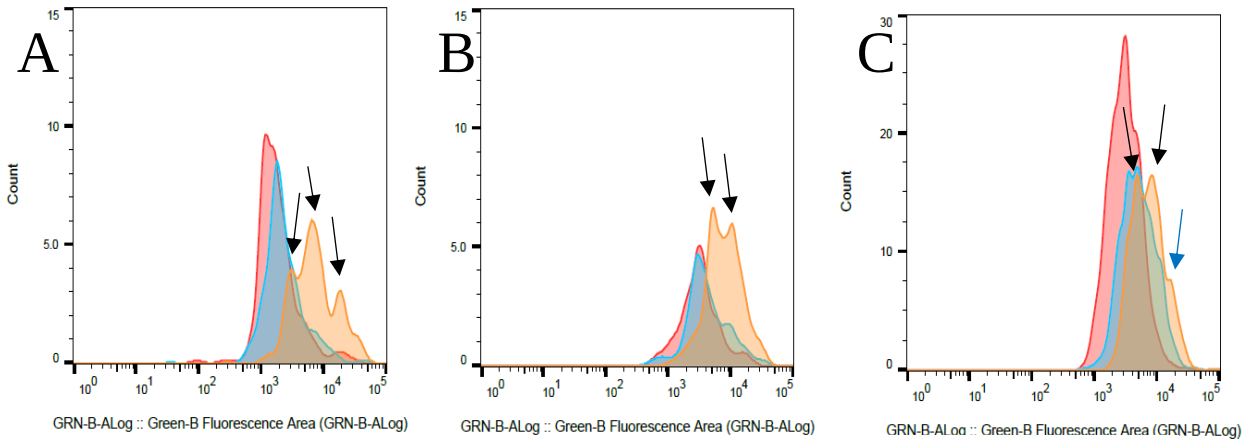

Figure 13 (A-C). Three-person mixtures. Unstained (red), isotype (blue), and anti-testosterone (orange). Distinguishable peaks are indicated by black arrows. **A.)** Three distinguishable peaks. **B.)** Two distinguishable peaks. **C.)** Two distinguishable peaks with a small shoulder on the right side indicated by a blue arrow.

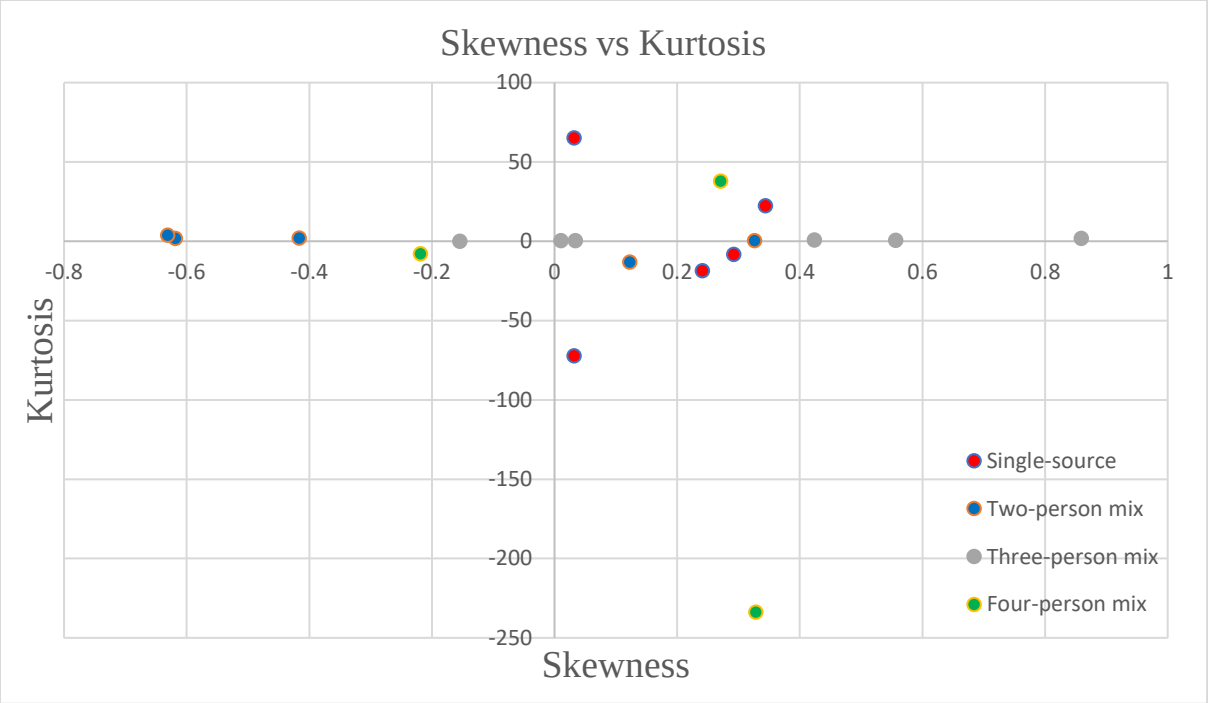

Figure 14. Scatterplot of the skewness and kurtosis of single-source samples (red, N=5), two-person (blue, N=5), three-person (gray, N=5), and four-person (green, N=3) mixtures. All single-source samples had a positive skewness value, whereas all of the mixtures showed samples with both positive and negative skewness values. Two- and three-person mixture samples consistently displayed kurtosis values very close to zero, whereas single-source samples and four-person mixtures displayed more variation in kurtosis.

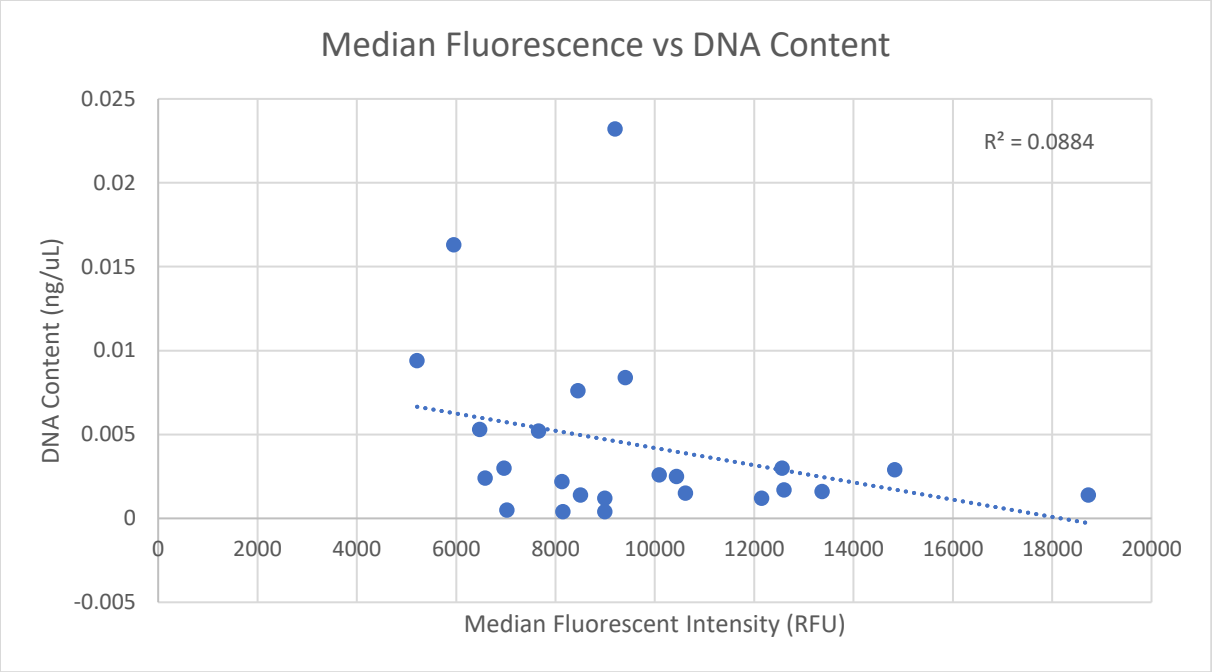

Figure 15. Median fluorescence (x-axis) from single-source samples plotted against DNA concentration (y-axis) of each sample. No correlation was observed.

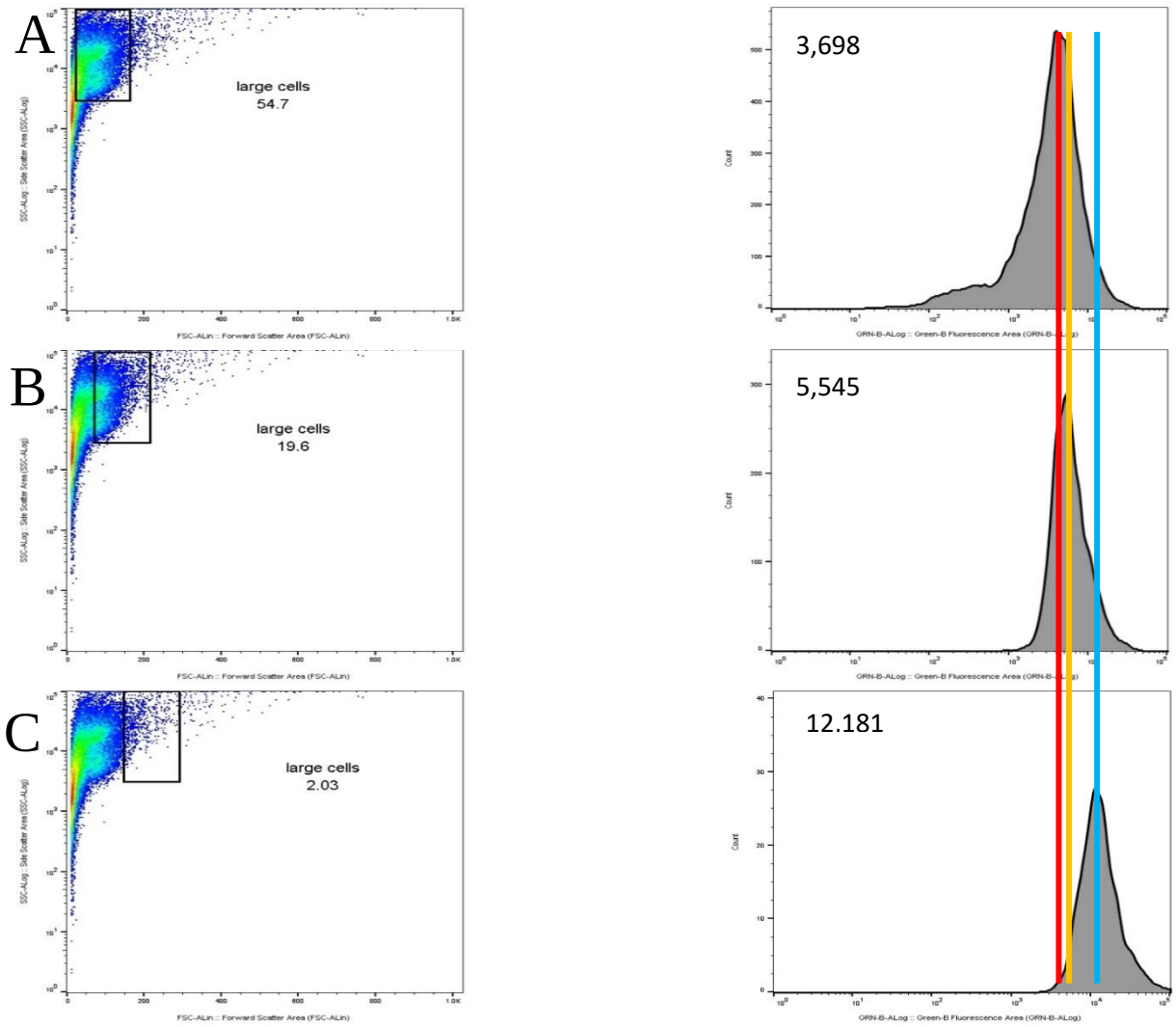

Figure 16 (A-C). Flow cytometry scatter plots on the left and fluorescence histograms of the gated events on the right. As the gate is shifted to the right to include only large and complex cells, the histogram shifts further to the right and becomes more symmetrical in shape. The median fluorescence values increase and are listed in the top left of each fluorescence histogram. The number underneath the large cells label in the scatterplots represents the percentage of the total events included within the gate. Each colored line is used to accentuate the differences in the median fluorescence as the gate is shifted to include larger and more complex cells.

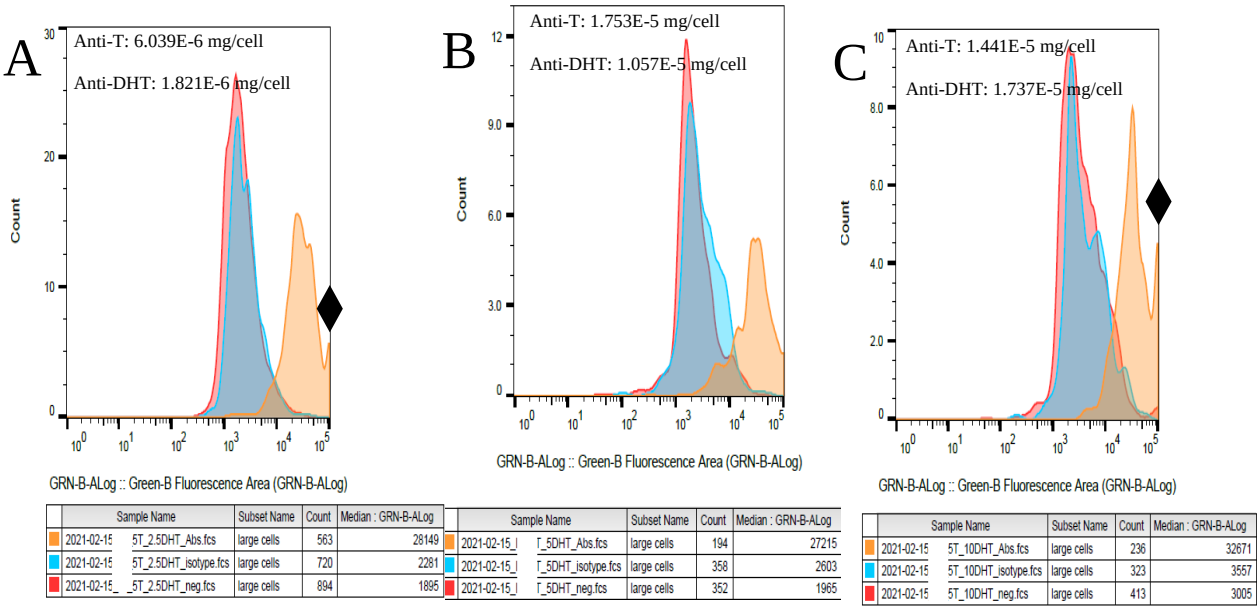

Sample Name	Subset Name	Count	Median : GRN-B-ALog
2021-02-15 5T_2.5DHT_Abs.fcs	large cells	563	28149
2021-02-15 5T_2.5DHT_isotype.fcs	large cells	720	2281
2021-02-15_ _5T_2.5DHT_neg.fcs	large cells	894	1895

Sample Name	Subset Name	Count	Median : GRN-B-ALog
2021-02-15_I T_5DHT_Abs.fcs	large cells	194	27215
2021-02-15_I T_5DHT_isotype.fcs	large cells	358	2603
2021-02-15_I T_5DHT_neg.fcs	large cells	352	1965

Sample Name	Subset Name	Count	Median : GRN-B-ALog
2021-02-15 5T_10DHT_Abs.fcs	large cells	236	32671
2021-02-15 5T_10DHT_isotype.fcs	large cells	323	3557
2021-02-15 5T_10DHT_neg.fcs	large cells	413	3005

Figure 17 (A-C). A single-source donor used to optimize the anti-T and anti-DHT antibodies together. Unstained (red), isotype (blue), anti-T and anti-DHT combination (orange). The amount of each antibody in mg/cell is listed within each histogram. The tail artifact is labeled with a black diamond. **A.)** 5 uL anti-T and 2.5 uL anti-DHT [0.0034 mg anti-T and 0.001025 mg anti-DHT]. **B.)** 5 uL anti-T and 5 uL anti-DHT [0.0034 mg anti-T and 0.00250 mg anti-DHT]. **C.)** 5 uL anti-T and 10 uL anti-DHT [0.0034 mg anti-T and 0.0041 mg anti-DHT].

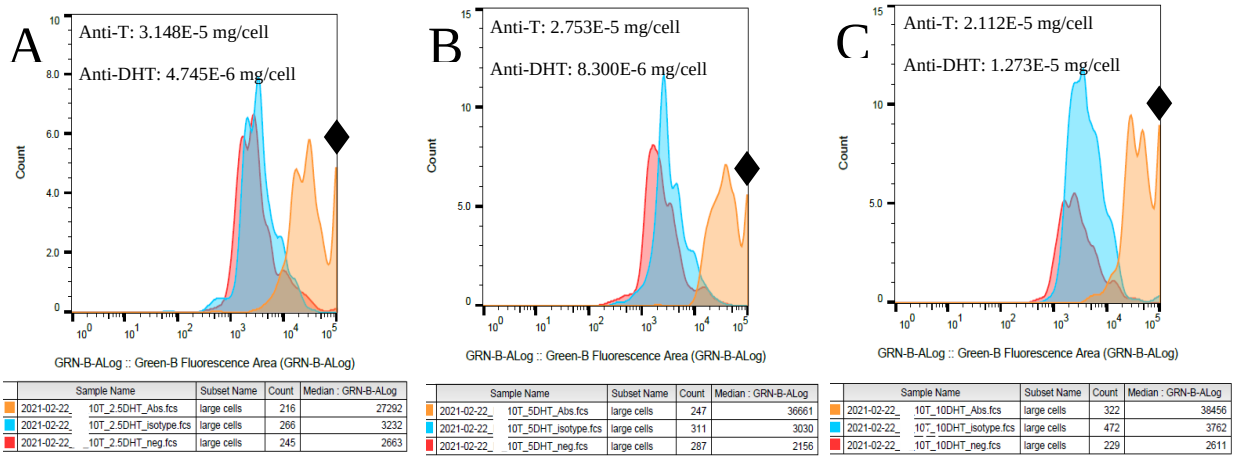

Sample Name	Subset Name	Count	Median : GRN-B-ALog
2021-02-22_ 10T_2.5DHT_Abs.fcs	large cells	216	27292
2021-02-22_ 10T_2.5DHT_isotype.fcs	large cells	266	3232
2021-02-22_ _10T_2.5DHT_neg.fcs	large cells	245	2663

Sample Name	Subset Name	Count	Median : GRN-B-ALog
2021-02-22_ 10T_5DHT_Abs.fcs	large cells	247	36661
2021-02-22_ 10T_5DHT_isotype.fcs	large cells	311	3030
2021-02-22_ 10T_5DHT_neg.fcs	large cells	287	2156

Sample Name	Subset Name	Count	Median : GRN-B-ALog
2021-02-22_ 10T_10DHT_Abs.fcs	large cells	322	38456
2021-02-22_ 10T_10DHT_isotype.fcs	large cells	472	3762
2021-02-22_ 10T_10DHT_neg.fcs	large cells	229	2611

Figure 18 (A-C). A single-source donor used to optimize the anti-T and anti-DHT antibodies together. Unstained (red), isotype (blue), anti-T and anti-DHT combination (orange). The amount of each antibody in mg/cell is listed within each histogram. The tail artifact is labeled with a black diamond. **A.)** 10 uL anti-T and 2.5 uL anti-DHT [0.0068 mg anti-T and 0.001025 mg anti-DHT]. **B.)** 10 uL anti-T and 5 uL anti-DHT [0.0068 mg anti-T and 0.00250 mg anti-DHT]. **C.)** 10 uL anti-T and10 uL anti-DHT [0.0017 mg anti-T and 0.0068 mg anti-DHT].

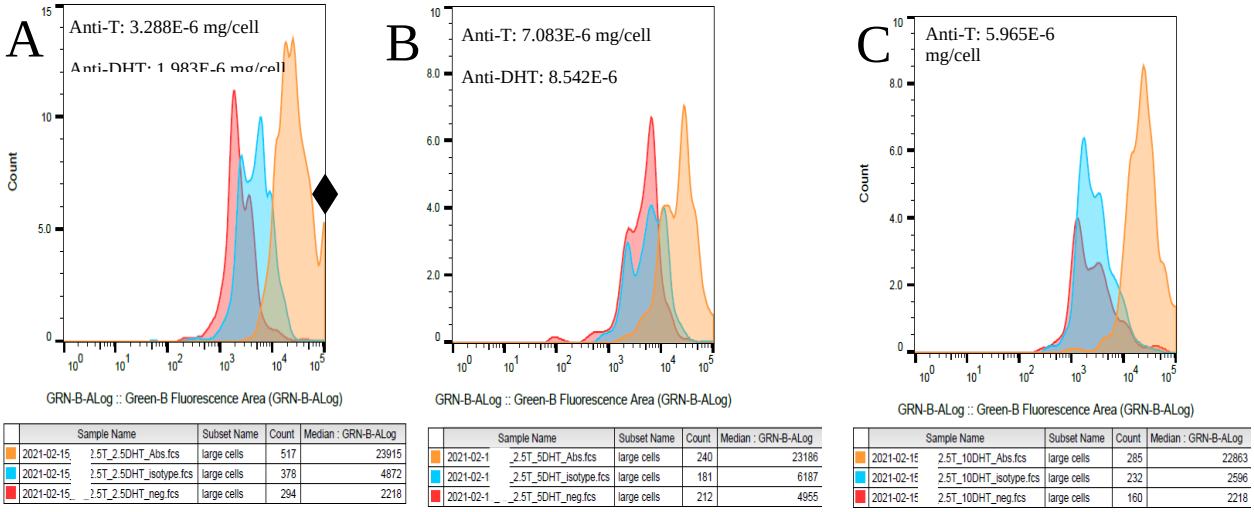

Sample Name	Subset Name	Count	Median : GRN-B-ALog
2021-02-15_ 2.5T_2.5DHT_Abs.fcs	large cells	517	23915
2021-02-15_ 2.5T_2.5DHT_isotype.fcs	large cells	378	4872
2021-02-15_ 2.5T_2.5DHT_neg.fcs	large cells	294	2218

Sample Name	Subset Name	Count	Median : GRN-B-ALog
2021-02-1 _2.5T_5DHT_Abs.fcs	large cells	240	23186
2021-02-1 _2.5T_5DHT_isotype.fcs	large cells	181	6187
2021-02-1 _2.5T_5DHT_neg.fcs	large cells	212	4955

Sample Name	Subset Name	Count	Median : GRN-B-ALog
2021-02-15 2.5T_10DHT_Abs.fcs	large cells	285	22863
2021-02-15 2.5T_10DHT_isotype.fcs	large cells	232	2596
2021-02-15 2.5T_10DHT_neg.fcs	large cells	160	2218

Figure 19 (A-C). A single-source donor used to optimize the anti-T and anti-DHT antibodies together. Unstained (red), isotype (blue), anti-T and anti-DHT combination (orange). The amount of each antibody in mg/cell is listed within each histogram. The tail artifact is labeled with a black diamond. **A.)** 2.5 uL anti-T and 2.5 uL anti-DHT [0.0017 mg anti-T and 0.001025 mg anti-DHT]. **B.)** 2.5 uL anti-T and 5 uL anti-DHT [0.0017 mg anti-T and 0.00250 mg anti-DHT]. **C.)** 2.5 uL anti-T and10 uL anti-DHT [0.0017 mg anti-T and 0.0041 mg anti-DHT].

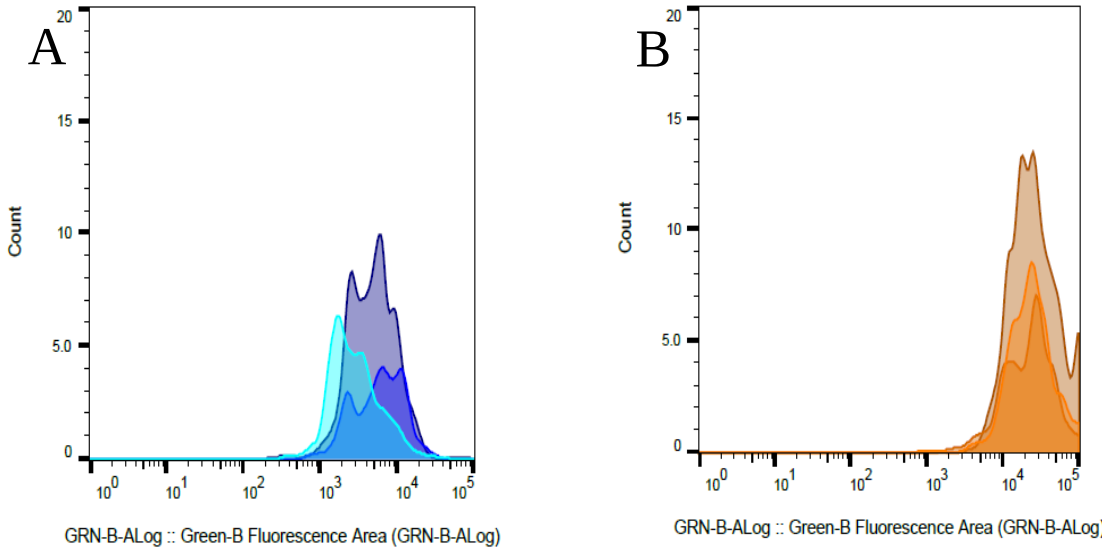

	Sample Name	Subset Name	Count	Median : GRN-B-ALog
	2021-02-15_ _2.5T_10DHT_isotype.fcs	large cells	232	2596
	2021-02-15_ _2.5T_5DHT_isotype.fcs	large cells	181	6187
	2021-02-15_ _2.5T_2.5DHT_isotype.fcs	large cells	378	4872

	Sample Name	Subset Name	Count	Median : GRN-B-ALog
	2021-02-15_ _2.5T_10DHT_Abs.fcs	large cells	285	22863
	2021-02-15_ _2.5T_5DHT_Abs.fcs	large cells	240	23186
	2021-02-15_ _2.5T_2.5DHT_Abs.fcs	large cells	517	23915

Figure 20. A.) Overlaid isotype control histograms for the combined 2.5 uL [0.0017 mg] anti-T and varied 2.5, 5, and 10 uL [0.001025, 0.00250, and 0.0041 mg] to show the differences in their fluorescence shifts. **B.)** Overlaid anti-T and anti-DHT histograms for the combined 2.5 uL [0.0017 mg] anti-T and varied 2.5, 5, and 10 uL [0.001025, 0.00250, and 0.0041 mg] to show the similarities in their fluorescence shifts.

Vita

Luke “Isaac” Baldridge was born on April 9, 1997, in Cleveland, Ohio. He graduated from Avon Lake High School in Avon Lake, Ohio in 2015. He received his Bachelor of Science in Cellular/Molecular Biology from Kent State University, Kent, Ohio in 2019. While pursuing his undergraduate degree, Isaac performed laboratory research in reproductive physiology as well as microbial ecology where his project focused on determining the abundance of cyanobacteria in Lake Erie that could degrade MC-LR liver toxins. While pursuing his graduate degree, Isaac was employed as a laboratory teaching assistant and became a Graduate Student Research Intern at the Virginia Department of Forensic Science to complete this thesis.